Universidade de Lisboa
Faculdade de Ciências
Departamento de Química e Bioquímica

Hydrogen peroxide modulation of angiogenic factors in tumor cells

Ana Maria Jerónimo Gameiro de Sousa

Dissertação
Mestrado em Bioquímica
(Especialização em Bioquímica Médica)

(2013)

Universidade de Lisboa
Faculdade de Ciências
Departamento de Química e Bioquímica

Hydrogen peroxide modulation of angiogenic factors in tumor cells

Ana Maria Jerónimo Gameiro de Sousa

Dissertação
Mestrado em Bioquímica
(Especialização em Bioquímica Médica)

Dissertação orientada pela Dra. Carla Real Afonso

(2013)

Table of Contents

Results

Discussion

FIGURE INDEX

TABLE INDEX

ACKNOWLEDGEMENTS

I would like to thank the following people for helping me and in some way greatly contributing in making this project come to fruition:

Carla Afonso, my supervisor for her guidance, patience, help, optimism and remarkable fighting spirit.

The other P.I.s of the GBOA group, particularly Luisa Cyrne, for extra help and discussion whenever needed.

Gonçalo Rodrigues for paving the way and then teaching me about his work.

Lara and Aida from the Fish Facility and Gabriel from microscopy for being amazing people and doing amazing work.

My lab companions Gonçalo, Mariana, Isabel and particularly Vânia for co-celebrating successes and co-commiserating on setbacks but always helping and cheering me on.

Filipe Vilas-Boas for the expertise, scientific advice and good nature that make him such a great person to work with.

Ana Bagulho, a kind, intelligent, extraordinary co-worker and even better person with whom I had the good fortune of sharing this adventure.

My friends, particularly Helga, Linda, Susana and Luís, and my extended family for enduring both my long absences and endless conversations and, despite them, always being supportive and encouraging.

J.A. and J.P. for bringing me joy and courage and being a guiding light all these years.

My brother Jerónimo, my sister Paula and my niece Andreia, the people I love the most.

My Dad who made all this possible though he was not here to see it. I hope I've made him proud.

To my Mom, for everything.

RESUMO

O desenvolvimento e disseminação de tumores sólidos dependem da formação de uma rede vascular que permita o aporte de oxigénio e nutrientes, através de um processo denominado angiogénese. Este processo é regulado por diversos factores que compõem o microambiente tumoral tais como os níveis de oxigénio, acidificação e stress oxidativo.

Sabe-se existir um nível elevado de espécies reactivas de oxigénio no microambiente tumoral que ao promover a desregulação de processos como a proliferação, a motilidade celular, a sobrevivência e angiogénese contribui para a iniciação, progressão e promoção tumoral.

Estudos realizados no nosso laboratório demonstraram que a diminuição dos níveis celulares de H_2O_2, através da sobreexpressão de catalase em células de carcinoma mamário de ratinho 4T1, leva a uma diminuição do recrutamento de células endoteliais e invasão vascular, num modelo de xenotransplante em peixe-zebra. O presente estudo pretende identificar os mecanismos moleculares dependentes do H_2O_2 responsáveis pela regulação da angiogénese. Para isso analisamos alterações na expressão de genes relacionados com o processo angiogénico em populações de células 4T1 com sobrexpressão de catalase através de transfecção transiente com um plasmídeo que permite a co-expressão de catalase e da proteína reporter mCherry.

A análise por PCR-array permitiu identificar vários alvos putativos do H_2O_2 incluindo efectores da via Notch e várias moléculas antiangiogénicas incluindo o inibidor de angiogénese específico de cérebro 1 (Bai1), a Trombospondina 1 (Thbs1) e o inibidor da metaloproteinase 3 (Timp3).

Foi observado por hibridação *in situ* que as células 4T1 expressam os ligandos Dll4 e Jagged1, o receptor Notch3 e o efector Hes1 mas a sua expressão parece ser independente da sobrexpressão de catálase.

Contrariamente aos componentes da via Notch, a expressão das proteínas Thbs1 e o Timp3 mostraram ser regulados pela sobreexpressão de catalase de uma forma não-autónoma e de uma forma autónoma, respectivamente. A baixa expressão de HIF-1α

nas condições experimentais deste trabalho indica que a regulação destas proteínas é independente deste factor de transcrição chave na regulação de factores reguladores da angiogénese. Verificou-se também que os níveis de expressão da proteína Bai1 nas células 4T1 são demasiado baixos impossibilitando os estudos subsequentes.

Os resultados obtidos neste trabalho mostraram que o nível de H_2O_2 nas células tumorais é capaz de regular a angiogénese através da modelação da expressão de moléculas anti-angiogénicas, de uma forma independente de HIF-1α.

Para além da regulação autónoma da expressão de proteínas pelo H_2O_2, efeito já observado anteriormente por outros autores, este trabalho revela que a alteração dos níveis de H_2O_2 numa subpopulação de células tumorais é capaz de condicionar a resposta angiogénica global através de um mecanismo não-autónomo. Assim o conhecimento dos mecanismos moleculares dependentes de H_2O_2 torna-se essencial para o desenvolvimento de terapias mais eficazes contra o cancro.

ABSTRACT

The development and dissemination of solid tumors depends upon the formation of a vascular network to supply oxygen and nutrients, through a process called angiogenesis. This process is regulated by several factors which are inherent to tumor microenvironment such as low oxygen levels, acidification and oxidative stress.

A high level of Reactive Oxygen Species is known to exist in tumor microenvironment which helps the dysregulation of processes such as proliferation, cell motility, survival and angiogenesis contributing to tumor initiation, progression and promotion.

Previous studies in our lab have demonstrated that lowering the cellular levels of H_2O_2 through overexpression of catalase in 4T1 mouse breast tumor cells, leads to a decrease in endothelial cell recruitment and tumor vessel invasion in a Zebrafish xenotransplant model.

The present study aims to identify H_2O_2 dependent molecular mechanisms responsible for angiogenesis regulation. We analyzed alterations in angiogenesis related gene expression in catalase overexpressing populations of the 4T1 cell line by transient transfection with a plasmid which allows co-expression of catalase and the mCherry reporter protein.

Through PCR-array analysis several putative H_2O_2 targets were identified including Notch pathway effectors and several antiagiogenic molecules including Brain-specific angiogenesis inhibitor 1 (Bai1), Thrombospondin 1 (Thbs1) and Tissue inhibitor of metalloproteinase 3 (Timp3).

Using *in situ* hybridization, we found that 4T1 tumor cells express the ligands Dll4 and Jagged1, the receptor Notch3 and effector Hes1 of the Notch pathway but their expression seems to be independent of catalase overexpression.

Unlike the Notch pathway components, the expression of Thbs1 and Timp3 were found to be regulated by catalase overexpression in a non-autonomous and an autonomous mode, respectively. The low expression of HIF-1α in the experimental conditions used in this work indicates that the regulation of these proteins is

independent from this key transcription factor in angiogenesis regulation. We found that Bai1 expression levels in 4T1 cells are too low to allow for subsequent studies.

The results obtained in this work have shown that the level of H_2O_2 in tumor cells is able to regulate angiogenesis in tumor cells through modulation of antiangiogenic molecules, in an HIF-1α independent manner.

Aside from autonomous regulation of protein expression by H_2O_2, previously described by several authors, this work shows that altering H_2O_2 levels in a subpopulation of tumor cells is enough to condition the overall angiogenic response through a non-autonomous mechanism. Thus, the understanding of H_2O_2 dependent molecular mechanisms is essential for developing more efficient antitumor therapies.

LIST OF ABBREVIATIONS

Ang-1	Angiopoietin 1
ANG-2	Angiopoietin 2
AP-1	Activator protein 1
ARE	Antioxidant response element
Bai1	brain-specific angiogenesis inhibitor 1
BCIP	5-Bromo-4-chloro-3-indolyl phosphate
bFGF	Basic fibroblast growth factor
BSA	Bovine Serum Albumin
CatO	Catalase overexpressing
CDX1	Caudal type homeobox 1
CM	Conditioned media
CSC	Cancer stem cll
DAPI	4',6-diamidino-2-phenylindole
Dll1	delta-like 1
Dll4	delta-like 4
DMEM	Dulbecco's Modified Eagle Medium
DTT	Dithiothreitol
EC	Endothelial cells
ECM	Extracellular matrix
EGF	Epidermal growth factor
ERK	Extracellular signal-regulated kinase
ERT2	estrogen receptor T2
ETC	electron transport chain
FAK	Focal Adhesion Kinase
FBS	Fetal Bovine Serum
GST	Glutathione S-transferase
Hes1	hairy and enhancer of split 1
Hes4	hairy and enhancer of split 4
Hes5	hairy and enhancer of split 5
Hes6	hairy and enhancer of split 6
Hey1	hairy/enhancer-of-split related with YRPW motif 1
Hey2	hairy/enhancer-of-split related with YRPW motif 2
HIF1	Hypoxia Inducible Factor 1
IkB	Inhibitor of kappa B
IL-1	Interleukin 1
IRES	Independent ribosome entry site
Jagg1	Jagged1
Keap1	Kelch ECH associating protein 1
MABT	Maleic acid buffer containing Tween 20
MAPK	Mitogen activated protein kinase
MMP	Matrix metalloproteinase
NADPH	Nicotinamide adenine dinucleotide phosphate (reduced)
NBT	Nitro blue tetrazolium chloride
NFkB	Nuclear factor kappa-light-chain-Enhancer of activated B cells
NLS	Nuclear localization sequence
Nox	NADPH oxidases
NQO1	NAD(P)H quinone reductase
Nrf2	Nuclear factor erythroid 2related factor 2
PBS	Phosphate Buffered Saline Solution
PBT	Phosphate buffered saline + Tween
pCIC	pCIC-IRES-mCherryNLS
pCIC-Cat	pCIC-Catalase-IRES-mCherryNLS
PDGF	Platelet-derived growth factor

PFA	Paraformaldehyde
PHD	Prolyl hydroxylase domain protein
PI3K	Phosphatidylinositide 3-kinases
Ptn	Pleiotrophin
PMSF	Phenylmethylsulfonyl fluorid
PTP	Protein tyrosine phosphatases
Rac1	Ras-related C3 botulinum toxin substrate 1
RNS	Reactive nitrogen species
ROS	Reactive oxigen species
RUNX3	Runt-related transcription factor 3
SDS-PAGE	Sodium dodecyl sulfate (SDS) Polyacrylamide gel electrophoresis
SOD	Superoxide dismutase
TAM	Tumor associated macrophages
TBS	Tris-buffered saline
Tdgf1	Teratocarcinoma derived growth factor 1
TGF- α	Transforming Growth Factor α
TGF- β1	Transforming Growth Factor β1
Thbs1	Thrombospondin 1
Timp3	Tissue inhibitor of metalloproteinase 3
TNF-α	Tumor necrosis factor α
VEGF	Vascular endothelial growth factor
VHL	von Hippel Lindau
vSMCs	vascular smooth muscle cells

OBJECTIVES

Previous results obtained in our laboratory (Rodrigues, G., Ms thesis, 2011) using the Zebrafish xenotransplantation model (Nicoli and Presta 2007) have shown that a decrease of H_2O_2 levels in tumor cells, due to transient catalase overexpression, impaired endothelial cell recruitment, vascular invasion and branching *in vivo*. These results raised the following questions:

- What are the angiogenic factors modulated by H_2O_2 in tumor cells?
- How is a small population of cells overexpressing catalase able to regulate tumor angiogenesis?

Therefore, the objectives of the present work are:

- Production of an expression vector for catalase that allowed the identification of the transfected tumor cells.
- Identification of angiogenic factors regulated by H_2O_2 in tumor cells.
- To understand whether the regulation of protein expression by H_2O_2 is cell-autonomous or non-autonomous.

Another goal of this work is to produce a Zebrafish transgenic line that allows the study of the role of H_2O_2 levels in endothelial cells during the angiogenic process. For that the specific aims are:

- Production of vectors for the inducible expression of catalase under the regulation of an endothelial cell specific promoter (Flk1).
- Injection of the vectors in one cell stage zebrafish embryos for transgenic production.

INTRODUCTION

THE ROLE OF REACTIVE OXYGEN SPECIES (ROS) IN CANCER

Cancer remains one of the most prevalent, deadliest and costly health issues in the world despite enormous efforts and significant achievements in cancer prevention, diagnosis, treatment and basic research.

Cancer statistics show that both the number of cases and mortality rate have been decreasing in the past few years in the United States of America (Siegel, Naishadham et al. 2012) but continue to increase worldwide and especially in developing countries (Jemal, Bray et al. 2011).

TUMOR MICROENVIRONMENT

Tumors are complex, heterogenic and dynamic structures consisting of three main components: tumor cells, tumor-associated cells and the extracellular matrix. Together they create an abnormal, interactive and evolving setting known as tumor microenvironment.

Malignant cells are associated with characteristics such as sustained proliferation, promotion of inflammation, genomic instability, resistance to cell death, altered metabolism, ability to evade growth suppressors and immune defenses, angiogenic potential and increased motility and migration leading to metastatic ability, known as the hallmarks of cancer (Hanahan and Weinberg 2011).

Tumor cells have various genetic modifications which include single mutations, amplification, loss or rearrangement of large regions of the genome leading to dominant gain of function and recessive loss of function in genes defined as oncogenes and tumor-suppressor genes, respectively (Sadikovic, B. et al 2008).

Cancers are thought to result from distinct subclones that are selected according to best adapted phenotypes from genetically and epigenetically diverse backgrounds. This heterogeneity exists not only in tumor cells but also in other components of the

tumor microenvironment resulting in a variability in tumor architecture with important implications for tumor development, diagnosis and treatment (Almendro, Marusyk et al. 2013).

Tumor-associated cells are cells which surround and interact with tumor cells contributing to tumor growth and dissemination. These include fibroblasts, immune cells, endothelial cells and other vasculature associated cells such as pericytes. .

Stromal cells contained in the tumor microenvironment are biologically active, adopting a myofibroblastic phenotype and contributing to extracellular matrix remodeling, cell proliferation and migration and angiogenesis induction by secreting tumor promoting factors such as proteinases. Because of the stroma-tumor cells interdependence, stromal cells can be used for cancer prognosis and are a potential therapeutic target (Franco, Shaw et al. 2010).

Vasculature cells present in the tumor microenvironment also behave abnormally creating a vascular network which while supplying nutrients and oxygen is also thought to promote tumor cell dissemination due to the aberrant permeability of tumor-associated vessels (Garcia-Roman and Zentella-Dehesa 2013).

Immune cells exist in high amounts in the tumor microenvironment and yet conversely do not eliminate tumor cells. Macrophages are the most abundant immune cell type found in tumors although tumor associated macrophages (TAMs) differentiate to the M2 type which are the main source of growth factors and cytokines (TGF-β1, PDGF, bFGF, TGF-α, TNF-α and IL-1) that promote angiogenesis, remodeling and tissue repair instead of M1 type which is associated with antitumor activity. Similarly, other immune cells help create an inflammatory and prooxidant microenvironment often likened to a perpetual wound (Dvorak 1986) (Coussens and Werb 2002) (Feng, Santoriello et al. 2010).

Besides cellular components, the tumor microenvironment is also constituted of several molecules that are dynamically regulated and play a crucial role in tumor maintenance and progression. The extracellular matrix (ECM) components are one of such examples. ECM is constituted by several proteins, such as collagen, fibronectin and laminin that are the basic components of basal membranes and function as a

substrate for cell adhesion and migration. Dysregulation of ECM homeostasis by the over expression of proteins responsible for the degradation and remodeling of ECM such as matrix metalloproteinases (MMPs), is a crucial event in cancer progression (Lu, Weaver et al. 2012). ECM sequesters proteases, cytokines, proteoglycans and growth factors which are inactive while imbedded in the matrix structure but can promote tumorigenesis upon matrix degradation.

Hypoxia, acidosis and oxidative stress are also part of the tumor microenvironment and are a consequence of tumor cell metabolism deregulation.

Tumor hypoxia has long been known to be an important feature of solid tumors and is attributed to a disorganized and inefficient vasculature that leads to hypoxic areas and fluctuations in O_2 levels (Bertout, Patel et al. 2008). Key factors in sensing and responding to hypoxia are the transcription factors hypoxia inducible factors (HIFs, including HIF1, HIF2 and HIF3) which are controlled by oxygen amount and oxidative state of cells. They are relevant to the expression of hundreds of genes involved in processes responsible for cell survival in low oxygen conditions, such as cell metabolism, angiogenesis, proliferation, motility and survival. HIF levels are found to be altered in several tumor types and relate to tumor angiogenesis, metastization and prognostic (Bertout, Patel et al. 2008, Keith, Johnson et al. 2012).

Acidosis in the tumor microenvironment (pH 5,6 to 6,8) is a characteristic of tumors while tumor cells maintain their intracellular pH neutral or alkaline (7.2 to 7.5) (Chiche, Brahimi-Horn et al. 2010). This acidification is generally attributed to the metabolic shift from oxidative phosphorylation to other metabolic pathways such as glycolysis and glutaminolysis as well as poor blood perfusion resulting in production of metabolic acids, such as lactic acid and their inefficient removal. Metabolic changes are driven by oncogenes as well as hypoxia and in turn acidosis promotes matrix degradation, death of surrounding normal cells and inhibits immune response to tumor cells (Gatenby, Gawlinski et al. 2006)

Together with hypoxia and acidosis, tumors have long been described to have higher oxidation levels than normal tissues due to accumulation of reactive oxygen species (ROS) and reactive nitrogen species (RNS). In cancer cells, the higher amounts of ROS promote changes that drive the tumorigenic process such as mutagenesis and

dysregulation of signaling pathways. However, due to an increase in the antioxidant response, cancer cells are able to adapt and overcome oxidative stress. Even though the thresholds for normal and cancer cells can differ considerably, all cells reach a point at which the ROS concentration is too high to allow cellular processes to continue and in these cases cells enter senescence or cell death occurs (Lopez-Lazaro 2007).

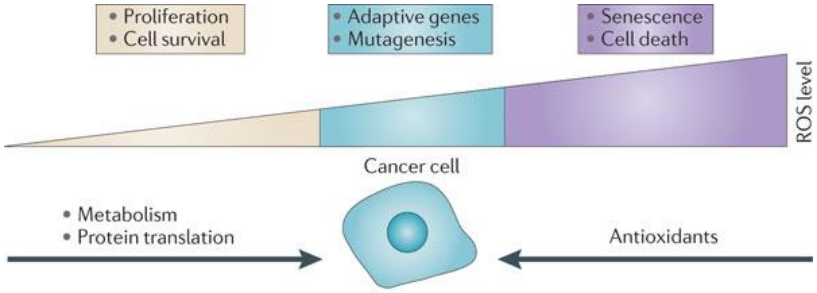

Fig.1: The different effects of ROS on cellular processes and their dependence on concentration (Cairns, Harris et al. 2011)

BIOLOGICAL FUNCTION OF ROS

Reactive oxygen species (ROS) is the term used to refer to a variety of reactive molecules containing oxygen.

There are two types of ROS: radicals, which contain one or more unpaired electron(s) in their outer molecular orbitals such as superoxide ($O_2^{\bullet-}$) nitric oxide ($NO^{\bullet-}$), hydroxyl ion ($OH^{\bullet}$) and peroxyl radicals (RO_2^-) and non-radical ROS, which do not have unpaired electron(s) but are chemically reactive and can be converted to radicals. These include, ozone (O_3), peroxynitrate (NO_4), and hydrogen peroxide (H_2O_2).

The formation of ROS in cells is mostly a natural consequence of the respiratory process. In the electron transport chain (ETC), during energy transduction, some electrons "leak" mostly at complexes I and III and react prematurely with molecules of O_2 forming superoxide anion. These highly reactive molecules react with other molecules to form the OH^- and H_2O_2 reactive species, among others (Drose and Brandt 2012). Aside from the mitochondrial ETC, ROS are produced by NADPH oxidases (Nox), the enzymes lipoxygenase and cyclooxygenase, xanthine oxidases, peroxidases and other hemoproteins, often in response to extracellular stimulus such as cytokines and

growth factors. ROS production can also result from external factors such as radiation or pollution.

The effects of ROS depend upon their concentration within cells. In normal cells, where a low steady-state concentration is maintained, many ROS act as signaling molecules interacting with cell components and contributing to fundamental processes such as cell proliferation and survival.

To avoid potential damage caused by oxidants, cells have an array of antioxidant molecules such as vitamins but the main line of defense is a system of antioxidant enzymes.

These include superoxide dismutases (SOD), such as MnSOD in the mitochondria and Cu/Zn SODs in the nucleus and cytosol that specifically dismutate the highly reactive $O_2^{\bullet -}$ into H_2O_2. Thioredoxins, peroxidases such as glutathione peroxidase and catalase reduce hydrogen peroxide to water.

The amount and localization of these enzymes is tightly controlled not only to avoid oxidative damage but also modulate signaling by ROS (Melo, Monteiro et al. 2011).

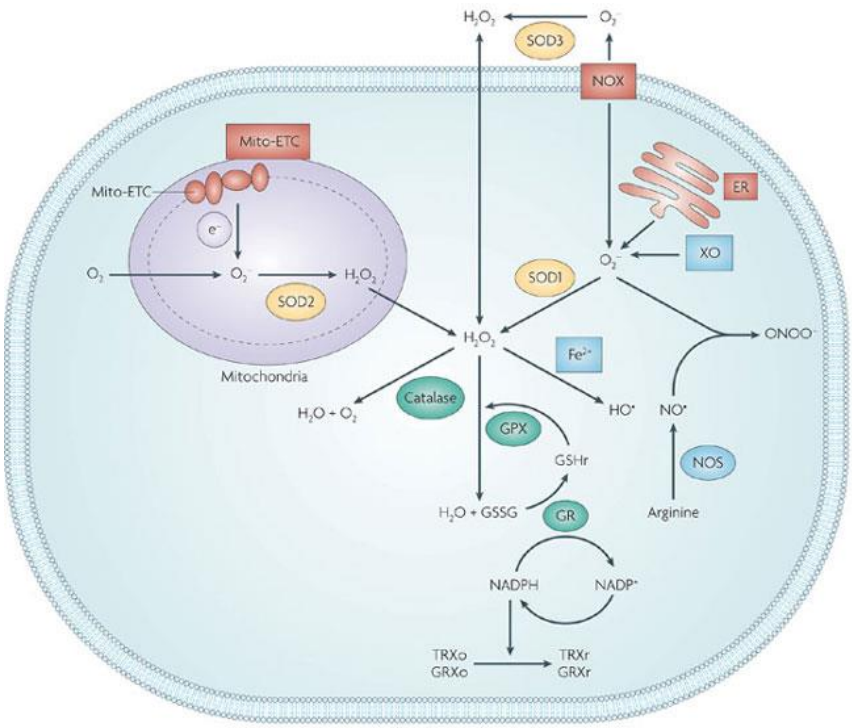

Fig. 2: Sites of cellular reactive oxygen species (ROS) generation (red) and major ROS-scavenging enzyme (yellow and green) (Trachootham, Alexandre et al. 2009)

The main regulator of cell response to oxidative stress is the Keap1-Nrf2 pathway where Nrf2 (nuclear factor erythroid 2-related factor 2) is a transcription factor that binds to the antioxidant response element (ARE) present in the regulatory regions of genes involved in redox homeostasis such as NAD(P)H quinone reductase (NQO1), glutathione S-transferase (GST), glutathione peroxidase, glutathione reductase and ferritin. Keap1 (Kelch ECH associating protein 1), is a cysteine-rich protein which is sensitive to redox environment and binds to Nrf2 leading to its proteossomal degradation. Oxidation of Keap1 is thought to change its conformation making it unable to bind to newly synthesized Nrf2 (Thimmulappa, Mai et al. 2002, Kansanen, Kuosmanen et al. 2013).

THE KEY ROLE OF H_2O_2

While more reactive species like OH^- can react indiscriminately and have short half lives, hydrogen peroxide presents characteristics that allow it to act as signaling molecule in a wide variety of pathways.

H_2O_2 is a weak oxidant with a relatively long cellular half-life (~1 ms, steady-state levels ~10^{-7} M) that reacts slowly with free metals, free glutathione and methionine residues but in contrast is very reactive with thiol groups of cysteine residues. The effect of H_2O_2 on its targets depends upon concentration, with possible reversible and irreversible reaction products. (D'Autreaux and Toledano 2007).

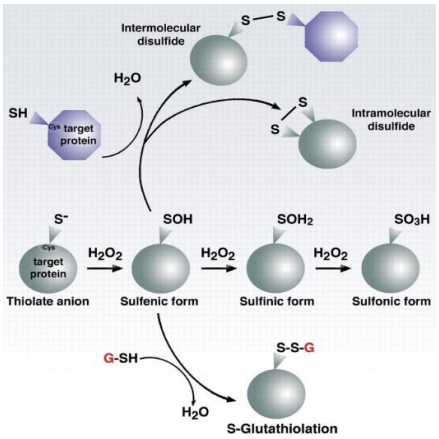

Fig. 3: Cysteine biochemistry allows for redox-dependent signalling by hydrogen peroxide (H_2O_2). An initial reaction with a thiolate yields sulfenic acid which can then further react originating reversible and irreversible products depending on H_2O_2 concentration (Finkel 2011)

H_2O_2 reacts directly with cysteine residues having pKa lower than 6 promoting the formation of disulfide bonds. These reactions can alter protein structure, affecting protein interactions and activities and happen in a temporal and sequence-specific manner.

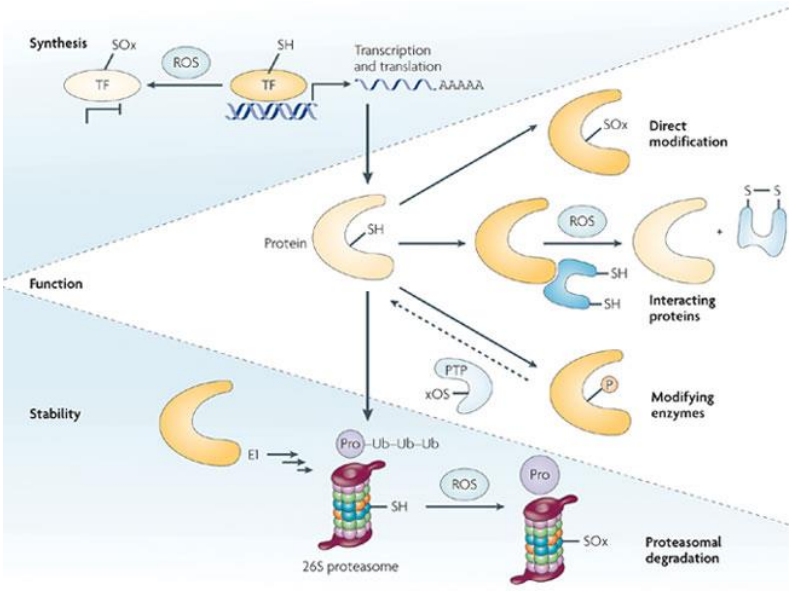

Fig. 4: Protein oxidation by ROS affects protein functions through multiple mechanisms. Oxidation levels can modulate transcription factors altering protein expression, can cause post-translational modifications that alter protein structure and reactivity, including modulating the activity of modifying enzymes such as phosphatases and can alter protein stability and subsequent degradation (Trachootham, Alexandre et al. 2009)

Although, unlike other ROS, H_2O_2 can diffuse through membranes and this diffusion might be modulated by changes in membrane permeability or by transport through aquaporins (D'Autreaux and Toledano 2007). The presence of H_2O_2 producing enzymes such as NADPH oxidases and H_2O_2 elimination enzymes such as catalase in specific cellular locations helps to modulate H_2O_2 concentrations and hence its reactivity within the cell (Finkel 2011).

REDOX REGULATION IN CANCER

ROS are known for having deleterious effects on cell components and increasing toxicity with higher concentrations, hence the necessity of antioxidant mechanisms within the cells.

"Oxidative stress' is an expression used to describe various deleterious processes resulting from an imbalance due to excessive formation of ROS and/or RNS and limited antioxidant defenses. Because of its widespread effects, oxidative stress is associated with many diseases such as cancer, Alzheimer's, diabetes and cardiovascular injuries (Waris G. and Ahsan H. 2006).

An increase in ROS in some tumor cells has been known to exist for a long time (Szatrowski and Nathan 1991) and its relation to tumor aggressiveness has been established in several tumors of which prostate cancer (Kumar, Koul et al. 2008), hepatocellular carcinoma (Suzuki, Imai et al. 2013), non-small cell lung carcinoma (Ceccarelli, Delfino et al. 2008) and pancreatic cancer (Kodydkova, Vavrova et al. 2013) are examples. However, an increase in markers of oxidative stress has been linked to better prognosis (Evans, Dizdaroglu et al. 2004, Karihtala, Kauppila et al. 2011) confirming that the relation between ROS levels and cancer is not yet understood.

Increasing ROS levels extracellularly or by genetic manipulation alters cell behavior as demonstrated by cell exposure to H_2O_2 sources increasing proliferation in epithelial cells (Sigaud, Evelson et al. 2005) and increasing mitochondrial ROS production via mutagenesis leading to metastatic behavior (Ishikawa, Takenaga et al. 2008)

Studies *in vitro* and *in vivo* have demonstrated that altering the levels of different ROS by overexpression of antioxidant enzymes, such as SODs and catalase or addition of reducing agents, also show effects in cancer development. Overexpression of copper zinc superoxide dismutase (CuZnSOD) (Zhang, Zhao et al. 2002) manganese SOD (MnSOD) and copper- zinc SOD (CuZnSOD)(Weydert, Waugh et al. 2006) have suppressive or delaying effects on tumor growth. ROS have also an important role in tumor microenvironment components such as endothelial and myeloid cells in which catalase overexpression reduces tumor aggressiveness *in vitro* (Glorieux, Dejeans et al. 2011) and *in vivo* (Goh, Enns et al. 2011)

In carcinogenesis, ROS have a decisive role due to a plethora of effects involved in tumor initiation, promotion and progression.

Genetic and epigenetic alterations

ROS, in particular hydroxyl radicals derived from H_2O_2 via Fenton reaction, have a role in tumor initiation by inducing direct damage to DNA, such as 8-hydroxy-2-deoxyguanosine (8-oxo-dG), the most common oxidation product of guanine which can give rise to G-to-T transversion mutations in key genes known to be involved in the development of cancer. An increase in 8-oxo-dG lesions in cellular DNA favors higher rates of mutation, leading over time to an increase in the risk for cancer (Ziech, Franco et al. 2011).

Aside from direct DNA damage, ROS have been implicated in gene regulation through epigenetic changes such a hypermethylation of promoter regions of tumor-suppressor genes like RUNX3 and CDX1 in colorectal cancer cells (Kang, Zhang et al. 2012, Zhang, Kang et al. 2013) and E-cadherin in hepatocellular carcinoma (Lim, Gu et al. 2008). In hepatocellular carcinoma, a tumor type strongly associated with oxidative stress, the expression of catalase is downregulated by prolonged exposure to ROS via promoter methylation, allegedly leading to a more aggressive phenotype (Min, Lim et al. 2010).

Another type of direct damage is chromosome instability which has been linked to oxidative stress, for instance in cells lacking SOD (Samper, Nicholls et al. 2003), and is a common feature of many cancers (Negrini, Gorgoulis et al. 2010).

Transcription factor expression and activity modulation

Several transcription factors involved in tumor-promoting gene expression are modulated by ROS.

Particular key transcription factors in tumors are the HIF protein family, which activate a large number of genes that are involved in cell survival processes in low oxygen conditions. HIF 1 is a heterodimer composed of HIF 1α and HIF 1β. HIF 1β is constitutively expressed while HIF 1α amount is tightly regulated through both protein synthesis and degradation.

HIF-1 synthesis is upregulated by growth factors in paracrine and autocrine fashions in an O_2 independent manner. Pathways involved in HIF transcription activation include mitogen-activated protein kinase (MAPK) and phosphatidylinositide 3-kinases (PI3K) and these can be disrupted in cancer cells through loss or gain-of-function of the proteins involved.

The degradation of HIF-1α is oxygen dependent, since its ubiquitination depends upon reactions where O_2 is a limiting reagent. In normoxia, the enzyme PHD (prolyl hydroxylase domain protein) 2 hydroxylates residues Proline 402 and Proline 562 in a reaction that converts 2-oxoglutarate to succinate. These PHDs require several cofactors, including 2-oxoglutarate, iron and ascorbate in addition to oxygen which supplies the oxygen atom for the hydroxyl group (Kaelin 2002).This hydroxylation allows the von Hippel Lindau (VHL) tumor suppressor protein to bind to HIF-1α followed by binding of ubiquitin3 which tags the protein for proteossomal degradation.

The level of ROS, specifically H_2O_2, within the cell can influence HIF-α synthesis through its modulation of the MAPK and PI3K pathways and can arguably also affect its degradation mechanism since hydrogen peroxide reacts with 2-oxoglutarate, Fe^{2+} and ascorbate and can thus limit Proline hydroxylation by PHDs (Qutub and Popel 2008).

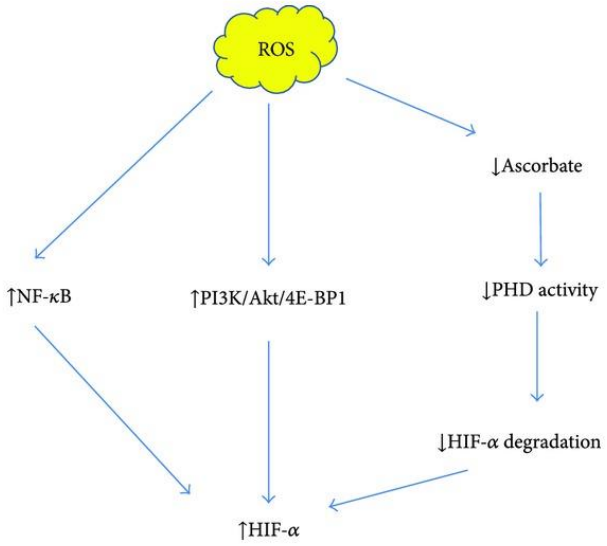

Fig. 5: ROS regulation of intracellular HIF 1α. Intracellular ROS modulate HIF 1α transcription via NF-*k*B and PI3K pathway activation as well as degradation by decreasing availability of PHD co-factors. (Zhou, Yan et al. 2013)

Also redox regulated is NFκB due to phosphorylation of the inhibitor I-κB which is mediated by oxidation. In addition the binding of the p50 subunit of NFkB to the DNA depends on reduction of an essential cysteine group (Katsuyuki, Kohzo et al. 1994) and is tightly regulated by H_2O_2 (Oliveira-Marques et al, 2009). NFκB activation can be triggered by oxidants in the absence of any physiological stimulus and is inhibited by a broad range chemically unrelated antioxidants (Flohe, Brigelius-Flohe et al. 1997). The

transcription factor AP-1 is also redox regulated since DNA biding depends on the reduction of cysteines in the subunits c-Jun and c-Fos (Abate, Patel et al. 1990).

Regulation of signal transduction

ROS are involved in several signal transduction cascades responsible for determining cellular proliferation or survival including the extracellular signal-regulated kinase (ERK) MAPK pathway, and the PI3K/Akt pathway. ROS induced dysregulation of these pathways may reduce cell dependence on growth factors.

The role of ROS in modulating signaling of these kinase pathways is largely attributed to reversible oxidative inactivation of protein tyrosine phosphatases (PTP), which inhibit signaling by dephosphorylating pathway components.

One of the first studies that established a direct connection between ROS and carcinogenesis is related to TGF-β signaling. TGF-β activation induces an increase in intracellular ROS in a process associated with the phosphorylation of Smad2, p38α and ERK1/2 (Rhyu, Yang et al. 2005). This molecular mechanism is required for tumor invasion and metastasis (McEarchern, Kobie et al. 2001)

In addition to these direct roles in intracellular signaling, the building up of local H_2O_2 gradients by modulation of antioxidant enzymes (Woo, Yim et al. 2010) affects other processes important to cancer promoting characteristics such as cell-to-cell adhesion (Goitre, Pergolizzi et al. 2012) and cytoskeletal reorganization (Jin, Lin et al. 2012) (Tochhawng, Deng et al. 2013).

The role of ROS in cancer and endothelial cells is determinant for the process of angiogenesis which is essential to tumor growth. Tumors produce many pro-angiogenic factors, such as vascular endothelial growth factor (VEGF), MMPs, angiopoietin-1, fibroblast growth factor (FGF), interleukin-8 (IL-8), platelet-derived growth factor (PDGF) and TGF-β. ROS are involved in the regulation of some of these factors, in particular VEGF, which is highly upregulated in most human cancers (Ferrara, Hillan et al. 2004).

ROS modulation of the tumor microenvironment

ROS are increased not only in tumor cells but also accumulate in tumor microenvironment since inflammatory response at the tumor site creates large amounts of ROS that are produced by activated neutrophils and macrophages.

ROS play an important part in the tumor microenvironment pro-inflammatory and pro-angiogenic features through pathways such as TGF-β signaling. TGF-β is a tumor environment modulator, due to the regulation of immune cell and fibroblast infiltration (Yang 2010). ROS also leads to the activation of MMPs via oxidation (Weiss, Peppin et al. 1985) that in turn increase mitochondrial ROS production by expression of an alternative splice product of Rac1 (Radisky, Levy et al. 2005). Another way in which stromal cells enable cancer cells oxidative stress is by supplying them with antioxidants as reportedly happens with bone-marrow-derived stromal cells which provide cysteine that enables leukaemia cells to resist oxidative stress (DeBerardinis 2012).

H_2O_2 has also been described as a possible chemoattractant for immune cells in wound repair (Niethammer, Grabher et al. 2009) and activator of macrophages (Owegi, Egot-Lemaire et al. 2010) with eventual implications for tumor microenvironment (Hurd, DeGennaro et al. 2012) .

Many proteins with relevance in cancer development can be altered through posttranslational modifications resulting from oxidative stress (Jorgenson, Zhong et al. 2013)

The plasmin protease is an example of redox regulation. It is activated by cleavage of its zymogen plasminogen and has a tumorigenic effect mainly through ECM degradation. However, plasmin is a precursor of angiostatin, an endogenous angiogenesis inhibitor. The cleavage of the N-terminal fragment of plasmin, which originates angiostatin, happens after reduction of 2 disulfide bonds and consequent conformational change (Cook and Hogg 2013).

ROS play a determinant part in cancer treatment as both radiation and several chemotherapy drugs increase oxidative stress since the high ROS content in cancer cells renders them more susceptible to oxidative stress–induced cell death (Fang, Nakamura et al. 2007). More recently however, the important role of therapy resistant

cancer stem cells (CSCs) in tumor relapse (Malik and Nie 2012) that present lower levels of ROS presumably due to more efficient antioxidant systems, has become the focus of cancer therapy research, highlighting once again the importance of redox regulation in cancer (Diehn, Cho et al. 2009).

TUMOR ANGIOGENESIS

Role of vasculature in cancer development

An adequate supply of oxygen and nutrients is critical for homeostasis of virtually all cells and tissues. The delivery of oxygen and nutrients, as well as the elimination of metabolic waste and carbon dioxide, occur through the vascular system, which is expanded by the processes of vasculogenesis and angiogenesis.

Tumors originate from small cellular masses with unchecked growth. As cells multiply both the oxygen and nutrients supplies needed for cell survival and proliferation become limiting leading to an equilibrium between cell proliferation and cell death. To grow beyond 1-2 mm in diameter and become a tumor this mass needs independent blood supply. This happens when cells acquire the capacity to induce blood vessel growth, in a process called tumor angiogenesis (Folkman 1974).

The existence of a tumor vasculature also helps cancer cells to enter the blood stream and spread to new locations leading to metastasis. In most cases the vascularization level of a solid tumor is thought to be an excellent indicator of its metastatic potential.
Formation of new blood vessels continues throughout tumor development being stimulated by pro-angiogenic factors especially in hypoxic tumor areas.
Another mechanism responsible for new vessel formation is called vasculogenesis. Vasculogenesis is the *de novo* formation of blood vessels through the differentiation of endothelial cell progenitors, the angioblasts (Risau and Flamme 1995). Although primarily important during development, post-natal vasculogenesis can also occur in the adult with bone marrow-derived endothelial progenitor cells being recruited to locations that present vascular stress, such as tumors.
Other mechanisms of vessel remodeling might also occur in tumors such as intussusception and vascular co-option (Carmeliet and Jain 2011), although these are less frequently described.

However, the predominant and better understood mechanism for new tumor vasculature formation is angiogenesis in which new blood vessels directed to the tumor mass sprout from pre-existing normal ones.

Mature vasculature consists of a system of tubes including arteries, arterioles, capillaries, venules and veins that promote the circulation of oxygenated blood between the heart, lungs and tissues (Herbert and Stainier 2011). The vessels in this network are formed by a monolayer of quiescent endothelial cells, interconnected by junctional molecules such as VE-cadherins and surrounded by vascular smooth muscle cells (vSMCs) or pericytes. vSMCs and pericytes are mesenchymal cell types with finger-like projections that wrap around vessel tubes. Their function is to stabilize blood vessels, contribute to the synthesis of vascular basement membrane that helps vessels withstand the pressure of blood flow and provide paracrine signaling essential to endothelium quiescence.

Molecular mechanism for vessel formation

Normal angiogenesis is a complex, highly regulated process (Herbert and Stainier 2011), involving a large number of pro-angiogenic and anti-angiogenic factors, consisting of the following main steps:

1. Angiogenic signaling and vessel destabilization

Quiescent endothelial cells receive angiogenic signals, such as VEGF, ANG-2, FGFs or chemokynes released by hypoxic, inflammatory or tumor cells, which activate endothelial cells inducing cell migration and proliferation.

The processes of endothelial cell migration and proliferation can only happen after basement membrane degradation and pericyte detachment from the capillary wall. This occurs by the action of extracellular proteinases known as matrix metalloproteinases (MMPs).

2. Tip cell selection and branching

The destabilization allows endothelial cell junctions to loosen, the vessel to dilate and the formation of a branch point. Proteinases degrade the matrix and remodel it to allow for endothelial cells migration and, at the same time, release angiogenic factors that are attached to the ECM, increasing the angiogenic stimulus. Integrins expressed by endothelial cells interact with specific components of the ECM, helping a directional migration.

Because not all cells can migrate equally, one cell is selected to lead the new vessel, named tip cell, while other cells, named stalk cells, follow and form the surface of the new vessel. The selection of the tip cell involves the notch signaling pathway, where the expression of notch ligands such as Delta like 4 and Jagged 1 in tip cells is detected by the notch receptors of neighboring cells that, as a result, repress production of molecules such as the VEGF receptor, effectively stopping them from becoming tip cells (Herbert and Stainier 2011).

Tip cells present specific characteristic such as high mobility, filopodia, increased sensitivity to angiogenic signals and high expression of VEGF receptor, which allow them to lead the branching of the new vessel in response to extracellular signaling.

3. Anastomosis and vessel stabilization

After endothelial cell proliferation in a given direction, the cells reorganize in order to form a tube structure with a central lumen with ANG-1 produced by the endothelial cells leading to vessel stabilization. New vessels then connect to reestablish the network and blood flow in a process known as anastomosis.

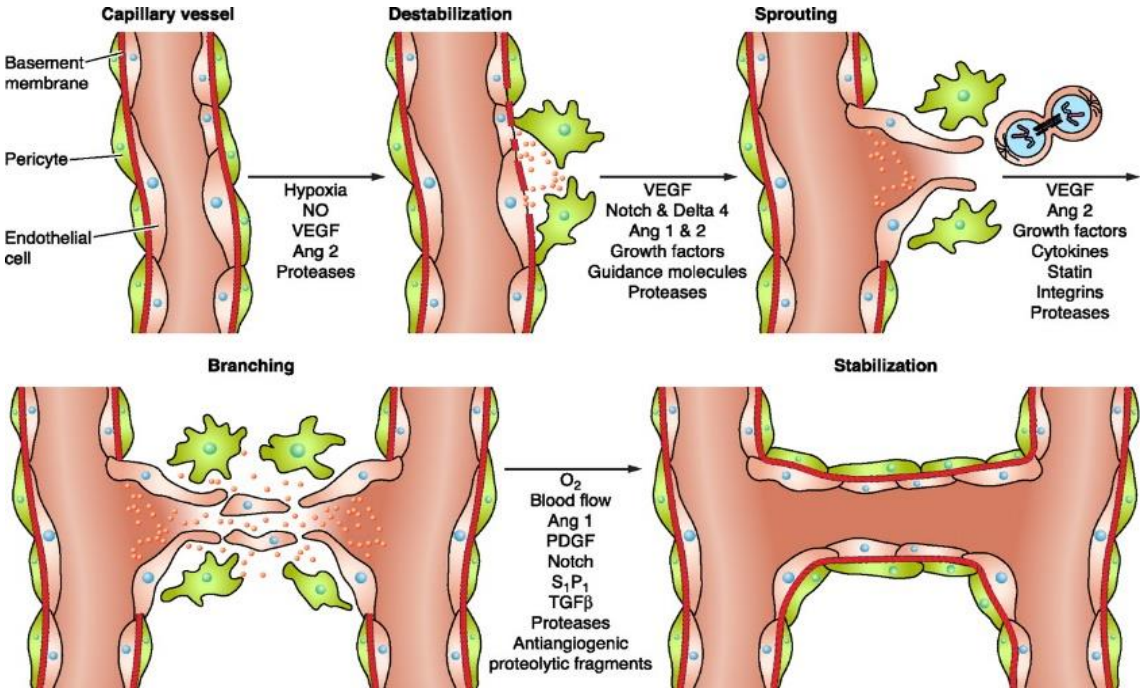

Fig. 6: The stages of angiogenesis: schematic representation of the steps in the angiogenic process as well as some of the main regulating factors involved (Clapp, Thebault et al. 2009).

In tumors, the angiogenic process is dependent on the activation of oncogenes, such as ras and c-myb, which upregulate pro-angiogenic factors or downregulate anti-angiogenic factors (Rak, Yu et al. 2000) . It is also dependent on signalling from components of the tumor microenvironment such as macrophages, fibroblasts and the extracellular matrix and it can be modulated by proteins in growth factors transduction pathways such as MAPK (Rousseau, Houle et al. 1997).

Role of H_2O_2 in angiogenesis

Reactive oxygen species, in particular superoxide and hydrogen peroxide, have long been known to be involved in cell proliferation and migration of different cell types since exogenous ROS addition in low concentrations stimulated migration and proliferation but did not induce cell death (Burdon 1995).

Additionally, studies in which ROS concentrations were lowered, either by blocking their production via the ETC or NADP(H) oxidases or promoting their degradation via antioxidant enzyme overexpression, have shown a decrease in cell migration, proliferation and adhesion due to disruption in signal transduction cascades (Brown, Miller et al. 1999), (Glorieux, Dejeans et al. 2011), (Goh, Enns et al. 2011).

An example is the vascular endothelial growth factor (VEGF) signaling pathway which controls multiple aspects of endothelial behavior such as endothelial differentiation, migration, proliferation, survival, and permeability (Ferrara, Gerber et al. 2003).

The best characterized ROS-modulated pathway involves the VEGF receptor 2 (VEGFR2, also called flt1 or KDR) signaling in endothelial cells. Although VEGF-A isoforms have a higher affinity for binding to VEGFR1, the tyrosine kinase activity of VEGFR2 is the main mediator of VEGF-A signaling during sprouting angiogenesis. This happens due to localized ROS induced inactivation of phosphatases, potentiating VEGFR2 phosphorylation.

Upon VEGF binding to VEGFR2, the small GTPase Rac1 is activated and translocates to the plasma membrane where it binds to the Nox2 subunit of NAD(P)H oxidase (Kao, Gianni et al. 2008), stimulating superoxide production and release into the extracellular medium. There this radical is dismutated to hydrogen peroxide which enters the cell through membrane diffusion or aquaporins situated near the VEGFR. The local increase in H_2O_2 leads to reversible oxidation and inactivation of protein tyrosine phosphatases (PTPs). While PTPs are inactive, VEGFR2 autophosphorylation is enhanced as well as downstream cSrc, FAK, PI3K and ERK signaling for which ROS are required, ultimately resulting in a stronger response from endothelial cells (Abid, Spokes et al. 2007).

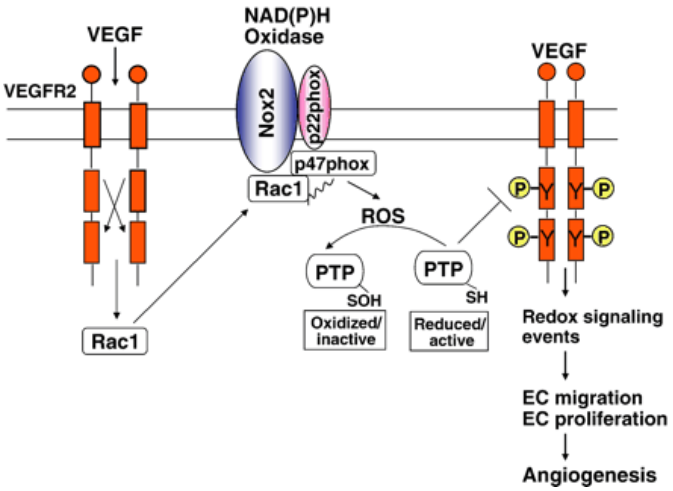

Fig. 7: ROS modulation of endothelial cell response to VEGF via NAD(P)H oxidase activation. VEGF binding to VEGFR2 activates Rac1 which binds to membrane bound NAD(P)H oxidases increasing ROS production. Reversible oxidative inactivation of Protein Tyrosine Phosphatases temporarily results in increased VEGFR2 autophosphorylation and VEGF signal reinforcement (Ushio-Fukai 2006).

Similar mechanisms exist to modulate signaling of other proangiogenic factors such as epidermal growth factor (EGF) (Truong and Carroll 2012), platelet-derived growth factor (PDGF) (Kang, Rhee et al. 2005) and angiopoietin1 (Harfouche, Malak et al. 2005).

ROS are also involved in the modulation of previously described pathways such as MAPK, PI3K, TGF-β (Wu 2006, Son, Cheong et al. 2011) and transcription factor regulation such as AP-1, NF-*κ*B and HIF1-*α*. These regulate other factors relevant in angiogenesis such as MMPs, MMPs natural inhibitors TIMPs and Notch pathway signaling (Zhou, Yan et al. 2013).

Despite the well-established relevance of ROS in cancer cells, endothelial cells and the tumor microenvironment, little is known about their role in interactions between different cell types. Specifically, the role of hydrogen peroxide as signaling molecule in a direct or indirect fashion is still incompletely understood.

THE ZEBRAFISH MODEL

Our study focuses on the effect of lowering H_2O_2 levels in cancer cells and endothelial cells on tumor angiogenesis.

The Zebrafish (*Danio rerio*) xenograft model was used to evaluate the effect of lowering H_2O_2 levels in cancer cells on the recruitment of endothelial cells. In further studies, we will study the effect of lowering H_2O_2 levels in endothelial cells on angiogenesis using transgenic Zebrafish.

Zebrafish presents many advantages as a model organism for the study of diseases. Zebrafish husbandry is comparatively easy in relation to other organisms and they can be obtained in large quantities. The embryos transparency and ex-utero development allow for phenotypic studies using non-invasive methods and xenografts are simplified due to immunoprivilege in the early stages of development. The organism is amenable to genetic manipulation with many genetic tools such as transposons, morpholinos and a large number of transgenic lines already in existence. The study of angiogenesis also benefits from detailed knowledge of Zebrafish vasculature and development as well as the similarities to humans in the molecular processes of vasculogenesis and angiogenesis, with angiogenic sprouting being easily visualized in Zebrafish embryos (Liu and Leach 2011) (Nicoli and Presta 2007)

MATERIALS AND METHODS

1. CELL CULTURE

All cell culture procedures were performed in a laminar flow hood (ClanLAF VFRS1206), using sterile disposable plasticware.

The 4T1 mouse mammary carcinoma cell line was used throughout this work. Cells were cultured as monolayers in high glucose Dulbecco's Modified Eagle Medium (DMEM) supplemented 100 units/ml penicillin, 100 µg/ml streptomycin, L-Glutamine 2 mM (referred to as DMEM unless otherwise specified) and 10% fetal bovine serum (FBS, inactivated at 56ºC for 20 minutes and filtered using a 25 µm filter) and maintained at 37°C in a humidified atmosphere containing 5% CO_2.

Cell passaging was done when cells reached approximately 80% confluence. Growth medium was removed and cells were washed twice with a 1x phosphate buffer saline (PBS) solution. A solution of trypsin 0,25% with 1 mM EDTA in 1xPBS was added so as to cover the monolayer and cells were incubated at 37ºC for a maximum of 3 minutes. Cells were then centrifuged at 169 g for 5 minutes and resuspended in growth media. The amount of cells seeded was determined after counting the cells in a hemocytometer.

2. TRANSFECTION OPTIMIZATION

Transfection of 4T1 cells was attempted by electroporation as well as using the cationic-lipid transfection reagents Lipofectamine® 2000 (Invitrogen) and Fugene® 6 (Promega). In order to estimate transfection efficiency the pCIC mCherry-NLS plasmid, containing the mCherry fluorescent protein, was used.

2.1 Electroporation

Cells were tripsinized at approximately 80% confluence, counted, resuspended in 400 µl of the appropriate medium (see table), placed in a 0,4 cm cuvette and electroporated using the Gene Pulser Xcell (BioRad) with the following conditions:

Number of cells	Medium	Wave type	Time (ms)	Voltage (V)
$5x10^5$	DMEM	Exponential	15	156
$5x10^5$	DMEM	Square	15,5	158
$5x10^5$	OptiMEM	Exponential	15	156
$5x10^5$	OptiMEM	Square	17,4	158
$5x10^5$	OptiMEM	Square	20	278
$5x10^5$	OptiMEM	Exponential	53,4	197
$5x10^5$	OptiMEM	Exponential	40,5	298
$5x10^5$	OptiMEM	Exponential	6	1491
$1x10^5$	OptiMEM	Exponential	6	1499

Table 1: Experimental conditions for electroporation of 4T1 cells.

Cells were plated in 24 well plates containing cover slips in DMEM complemented with 10% FBS and incubated at 37ºC, 5% CO_2 for 14-18 hours.

2.2 Lipid transfection reagents

The reagents lipofectamine 2000® (Invitrogen) and FuGENE 6® (Promega) were tested. Cells were seeded in 96 or 24 well plates at different densities (see table 2 below) in DMEM complemented with 10% FBS but no antibiotics 16-20 hours before transfection.

Different ratios of reagent:DNA were used (see table 2 below) and transfection was tested by diluting lipofectamine and DNA in the quantities below in 1:8 final cell culture volume of OptiMEM® each in separate tubes in Opti-MEM media (Invitrogen) and let stand for 5 minutes as room temperate. The lipofectamine and DNA solutions were then gently mixed together and left at room temperature for 20 minutes to allow for formation of lipofectamine:DNA complexes and the mix was gently distributed over the cells. FuGENE 6 in the quantities specified below was mixed in 1:10 final cell culture volume of OptiMEM® and incubated for 5 minutes. Next the appropriate amount of DNA was added to this solution, mixed and incubated for 15 minutes. The mix was then gently added to the cell culture.

Cell density (cells/cm^2)	Lipofectamine:DNA (µl/µg) per ml cell culture	Fugene:DNA (µl/µg) per ml cell culture
1,5x10^5	2,5:2,5	5:2,5
	5:2,5	7,5:2,5
	10:2,5	15:2,5
2,5x10^5	2,5:2,5	5:2,5
	5:2,5	7,5:2,5
	10:2,5	15:2,5
5x10^5	2,5:2,5	5:2,5
	5:2,5	7,5:2,5
	10:2,5	15:2,5

Table 2: Experimental conditions for transfection of 4T1 cells with lipid reagents.

Cells were incubated for a further 24 hours before transfection efficiency was determined.

2.3 Transfection efficiency determination

Preliminary tests were performed in 96 well plates and comparative transfection efficiency was done by measuring mCherry using a SpectraMax Gemini fluorometer.

Conditions with best results were then tested in 24 well plates with cover slips and transfection efficiency was determined using fluorescence microscopy. Briefly, cells were washed with PBS, fixed in 4%PFA (paraformaldehyde) for 30 minutes and again washed with PBS. DAPI (4',6-diamidino-2-phenylindole) was added at 1 µg/ml, left for 5 minutes and cells were again washed with PBS. Fixed cells were stored in PBS at 4ºC in the dark.

The coverslips were mounted on a lamella with mowiol® (Sigma-Aldrich) and cells were observed using an Olympus BX60 microscope with 20x amplification. Random sections were photographed and number of transfected and total cells was counted using 4 photographs for each condition (ImageJ software) and transfection efficiency calculated.

3. Cell transfection

After optimization it was determined that the most efficient transfection method was using Lipofectamine® 2000 (Invitrogen) as described below.

Cells were seeded at a density of $2{,}5x10^4/cm^2$ approximately 16 hours before transfection in DMEM complemented with 10% FBS but no antibiotics. Lipofectamine was diluted 1:50 and DNA was diluted to 20 µg/µl in separate tubes in Opti-MEM and let stand for 5 minutes as room temperate. The lipofectamine was gently mixed with the DNA in a 1 µl lipofectamine to 1 µg DNA proportion and left at room temperature for 20 minutes. This mix was then added to the cells in FBS and antibiotic free DMEM media as the process of transfection is inhibited by these additives. After approximately 7 hours the transfection media was replaced by DMEM containing penicillin and streptomycin and complemented with 10% FBS. Cells were maintained for 24 hours before subsequent experiments to allow for the expression of the proteins of interest.

4. Native gel catalase activity assay

Activity of exogenous catalase was observed using a non-denaturing polyacrylamide gel to separate the native protein followed by coloring with potassium ferrocyanide and ferric chloride, which react only in the presence of peroxide to form the precipitate Prussian Blue (Weydert and Cullen 2010).

4.1 Protein extraction

HeLa cells were transfected as described above with control and catalase plasmid in 6-well plates, with a transfection efficiency of 40-45%, and total protein was extracted at different time points after transfection: 8 hours, 16 hours and 24 hours.

Cells were washed with PBS, scraped with the aid of a rubber policeman and centrifuged for 5 min at 200g, 4 °C. The supernatant was removed the cells resuspended 50 µl of 50 mM phosphate buffer (PB, pH 7.8). Cells were sonicated on

ice 3 times for 2 minutes with 30 seconds intervals using a Sonorex TK52 sonicator. Cell pellets were stored at − 20 °C until assayed.

4.2 Protein quantification

The concentration of protein present in cellular extracts was determined using the standard Bradford protein assay. This assay is based on the shift observed in the absorption maximum of the Brilliant Blue G-250 dye upon its binding to protein as described by Bradford M. (Bradford 1976).

A calibration curve was made using standard solutions of known concentration of Bovine Serum Albumin (BSA) between 0,1 µg/µl and 1,25 µg/µl. In 96-well plates, 250 µl of Bradford reagent (Sigma) were added to 5 µl of standards, samples or distilled water (blank) in triplicate and the mix was incubated in darkness for 30 minutes with gentle agitation. Absorbance at 595 nm was then read in a microplate reader (Tecan Sunrise).

4.3 Protein separation by polyacrylamide native gel

Native polyacrylamide gels consisting of an 8% separating gel topped by an 5% stacking gel were prepared in a protean apparatus (Biorad) with 1,5 mm spacers using the following quantities:

Reagent	Volume for 8% separating gel	Volume for 5% stacking gel
ddH2O	10,95 ml	-
Acyl-Bis 30% (wt/vol)	4,8 ml	1 ml
Tris separating buffer pH 8.8	2,25 ml	-
Tris stacking buffer pH 6.8	-	2,4 ml
Sucrose 40% (wt/vol)	-	3,2 ml
TEMED	9 µl	4 µl
APS 10% (wt/vol)	68 µl	40 µl

Table 3: Composition of native polyacrylamide gels for native gel catalase activity assay.

The gel was first run in pre-electrophoresis buffer for 1 h, at 40 mA at 4 °C to remove gel components that may inactivate proteins. After this run, samples were loaded. For each sample a total of 20 µg was used, applied diluted 1:1 in sample loading. Positive controls of 100 mU, 1 U and 2 U bovine liver catalase were used. Samples were run in

the pre-electrophoresis buffer for 3 h at 40 mA at 4 °C. The pre-electrophoresis buffer was then replaced by electrophoresis buffer and the gel run in the same conditions for approximately another 3 hours, stopping 1 hour after the dye front reached the gel bottom.

4.4 Gel staining

The gel was washed in distilled water three times for 10 minutes each time and then incubated in a 0,003% H_2O_2 solution for 10 minutes. After rinsing twice with distilled water for 5 minutes, the two staining solutions of ferric chloride (2% (wt/vol)) and potassium ferricyanide (2% (wt/vol)) were added simultaneously.

In the areas where H_2O_2 is present the following reaction occurs:

$2\ K_4FeC_6N_6 + H_2O_2$ -----> $2\ K_3Fe(CN)_6 + 2\ KOH$

The resulting ferrocyanide then reacts with ferric chloride:

$4\ FeCl_3 + 3\ K_4Fe(CN)_6$ -----> $Fe_4[Fe(CN)_6]_3 + 12\ KCl$

The resulting compound, known as Prussian Blue, forms a precipitate that covers the gel except in the areas where catalase activity has depleted H_2O_2, forming achromatic bands proportionate to catalase activity. After these bands have appeared, the stain was removed and the gel was rinsed several times with distilled water and left at room temperature for 18–24 h in distilled water under ambient light to allow for further band development.

Gels were scanned and band size and intensity compared using ImageJ software.

5. HIF 1α EXPRESSION QUANTIFICATION

We compared HIF 1-α expression in protein extracts from 4T1 cells in the following conditions:

- Control cells incubated for 16 hours in normoxia followed by 8 hours in hypoxia (5% oxygen)

- Catalase transfected cells incubated for 16 hours in normoxia followed by 8 hours in hypoxia (5% oxygen)
- Control cells incubated for 24 hours in normoxia (21% oxygen)

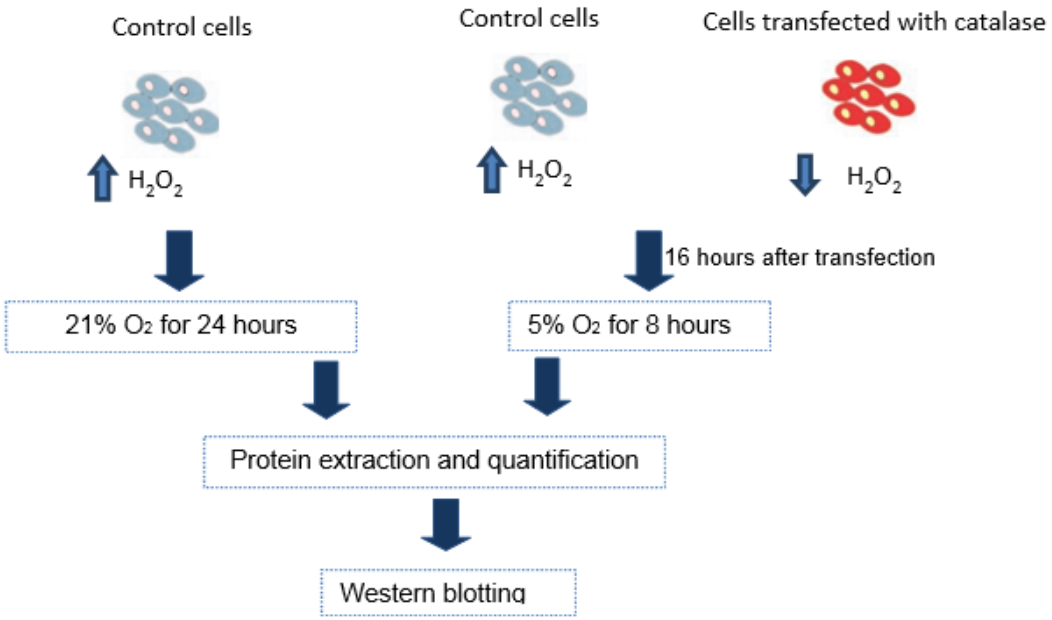

Fig. 8: Experimental design for quantification of HIF 1α in normoxia and hypoxia.

5.1 Protein extraction

To obtain an extract of whole cell protein, the RIPA lysis and extraction buffer was used, complemented with protease inhibitors to minimized protein degradation.

Cell culture dishes were placed on ice, cell growth media was removed and cells were washed with ice-cold PBS. Cells were scraped from the dish using a rubber policeman in approximately 10 µl/cm^2 growth area of PBS and remaining cells were washed from the surface using the same amount of PBS. The collected cells were centrifuged at 5000 g, 4ºC for 5 minutes. The supernatant was removed and cells were resuspended in RIPA lysis buffer in the presence of protease inhibitors (benzamidin, leupeptin, pepstatin, PMSF and DTT) and incubated on ice for 10 minutes. The lysate was then centrifuged at 15000g, 4ºC for 15 minutes. The supernatant containing the protein extract was collected and stored at −80 °C.

Protein was quantified as described in section 4.2.

5.2 Immunoblotting

Immunoblotting makes use of antibodies to bind and visualize a specific protein in a protein extract after it has been subjected to separation by polyacrylamide gel electrophoresis.

Equal amounts of proteins (40-70 µg) from each sample and 4 µl of loading buffer were mixed and distilled water was added to a final volume of 30 µl. The LMW protein ladder (GE Healthcare) was used to determine protein sizes.

Samples were heated at 90ºC for 5 minutes and then loaded onto a polyacrylamide gel consisting of 5% stacking gel and 8% separating gel (Maniatis, Fritsch et al. 1982). The gel was run at 100 V in running buffer for approximately 80 minutes.

Gels were equilibrated in transfer solution and electroblotted to nitrocellulose membranes using semi-dry blot transfer cell (BioRad) for 1 hour at 2 mA/cm^2 of membrane.

Protein transfer was observed by coloring the membrane with Ponceau solution. The membranes were then blocked for 1 h in TBS buffer (pH 7.4) containing 0.1% Tween-20 (Sigma) and 3% powdered milk protein and then incubated overnight at 4 °C with the HIF 1α antibody (MAB1536 from R&D systems) diluted 1:500 in blocking solution. Membranes were washed three times with TBS containing 0.1% Tween-20 (Sigma) and incubated for two hours with a 1:5000 dilution of secondary antibody coupled to horseradish peroxidase in TBS containing 0.1% Tween-20 and 3% powdered milk protein. Protein bands were then detected by chemiluminescence, using the ECL Prime detection kit from GE healthcare and visualized using Imagequant LAS 500 (GE healthcare).

6. Analysis of gene expression using quantitative RT-PCR

Gene expression in control and cell populations transfected with exogenous catalase was compared by extracting total RNA, synthesizing cDNA and performing quantitative real-time PCR.

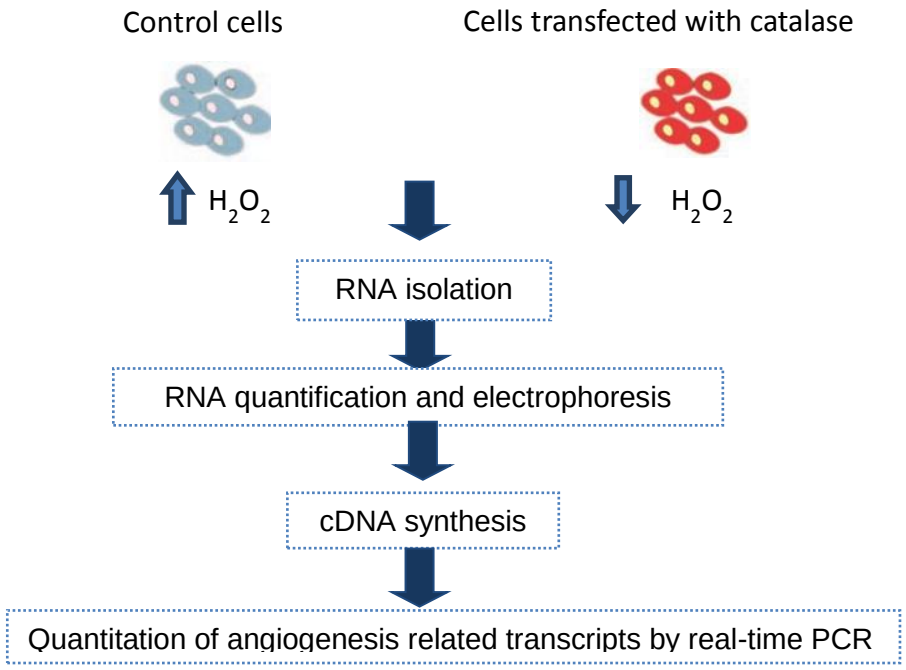

Fig. 9: Experimental design for gene array analysis of control and catalase transfected cell populations.

6.1 RNA extraction

Total RNA extraction was performed using Trizol reagent (Invitrogen) following manufacturers' instructions. Briefly, cells were washed with ice cold PBS and Trizol was added (1 ml/20 cm^2 of cell culture plate). Cells were lysed by pipetting and the mixture was incubated at room temperature for 5 minutes. Then chloroform was added at a ratio of 0.2 ml/(ml of Trizol) and tubes were vortexed vigorously for approximately 15 seconds and left at room temperature for another 3 minutes. This was followed by centrifugation at 12000 g for 15 minutes at 4ºC to obtain phase separation. The aqueous phase (supernatant) containing the RNA was carefully removed to a new tube and isopropanol was added at a rate of 0.5 ml/(ml of Trizol) to precipitate RNA. Solution was mixed by gentle inversion and left at room temperature for 10 minutes. This was followed by centrifugation at 12000 g for 10 minutes at 4ºC to obtain the RNA pellet. The pellet was washed using 1 ml of ethanol 75% followed by centrifugation at 7500g for 5 minutes at 4ºC. All supernatant was removed and the pellet was let dry for a few minutes before being resuspended in nuclease-free water.

Genomic DNA was eliminated by digestion with DNAse (Thermo Scientific). The following reagents were added and the mix incubated at 37ºC for 30 minutes.

Reagent	Quantity
DNAse buffer (10x)	3 µl
RNA	1 µg
RiboLock, RNAse inhibitor (20 U/µl)	1 µl
DNAse (1 U/µl)	3 µl
ddH_2O, nuclease-free	To 30 µl

Table 4: Reagents used for DNA digestion in total RNA extracts.

After incubation, 3 µl of 50 mM EDTA were added followed by an incubation at 65ºC for 10 minutes to inactivate the DNAse.

RNA was quantified using Nanodrop 1000-1000 and its integrity observed in 1% agarose gel.

A PCR for a house-keeping GAPDH gene sequence was used to ascertain there was no residual genomic DNA contamination.

For each sample plus a negative (containing water) and a positive (containing mouse cDNA) controls the following reagents were used:

Reagent	Quantity
DreamTaq polymerase buffer (10x)	2 µl
dNTPs (10 mM)	2 µl
Forward Primer for GAPDH (10 µM) (ThermoScientific)	0,2 µl
Reverse Primer for GAPDH (10 µM) (ThermoScientific)	0,2 µl
RNA	200 µg
DreamTaq polymerase (5U/µl) (ThermoScientific)	0,25 µl
ddH_2O, nuclease-free	To 20 µl

Table 5: Reagents used for PCR for the house-keeping gene GAPDH to verify there is no DNA contamination in total RNA extracts.

The PCR program (in a PTC-100 thermocycler) used was:

Denaturation	95ºC	5 min
Denaturation	95ºC	1 min
Annealing	60ºC	1 min 30s
Extension	72ºC	1 min
Extension	72ºC	10 min

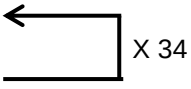

PCR products were visualized in 1% agarose gel.

6.2 cDNA synthesis

cDNA was obtained from extracted RNA using the RevertAid H minus first strand cDNA synthesis kit (Thermo scientific) according to manufacturer's instructions.

For each sample plus a negative (containing water) and a positive (GAPDH RNA) controls the following reagents were used:

Reagent	Quantity
RNA	0,5 µg
Random hexamer primer	1 µl
Reaction Buffer (5x)	4 µl
dNTPs (10 mM)	2 µl
RiboLock RNase Inhibitor (20 U/µl)	2 µl
RevertAid H Minus M-MuLV Reverse Transcriptase (200 U/µl)	1 µl
ddH_2O, nuclease-free	To 20 µl

Table 6: Reagents used for cDNA synthesis from total RNA extracts using the RevertAid H minus first strand cDNA synthesis kit (Thermo scientific).

Reaction tubes were placed in a thermocycler and incubated at 25ºC for 5 minutes to allow for random primer annealing, 50ºC for 30 minutes for cDNA synthesis and finally at 85ºC for 5 minutes to inactivate the enzyme, thus stopping the reaction.

cDNA was stored at -20ºC until use.

6.3 Real Time RT-PCR

Real time reverse-transcriptase PCR is used to quantify the RNA amplified by a given set of primers in comparison to a control one. This allows for a quantitative comparison of gene expression in a set of different RNA samples, after normalization using an equally expressed control gene sequence. The addition of SYBR Green, which emits fluorescence after binding to double stranded DNA allows us to follow the quantity of PCR product amplified, which correlates with the initial RNA present in the sample.

We used Real Time RT-PCR to compare cDNAs obtained from our control plasmid transfected cells and from our catalase plasmid transfected cells. The RT² Angiogenesis Profiler™ PCR Array System for mouse by SABiosciences, which compares the expression of 84 genes involved in modulating the biological processes of

angiogenesis, including growth factors, receptors, transcription factors, cytokines and matrix related proteins in a total of 4 samples was used for the initial screening.

One control cDNA combining 500 µg RNA from 3 different control samples was compared with 3 cDNAs from 3 different catalase containing samples. Original cDNAs were diluted 1:6 using nuclease-free MQ water. Mixes were prepared as per manufacturers' instructions:

Components	Volume (µl)
2X SABiosciences RT2 qPCR Master Mix	550
Diluted First Strand cDNA Synthesis Reaction	102
ddH_2O	448
Total Volume	1100

Table 7: Reagents used for gene array analysis using the RT² Angiogenesis Profiler™ PCR Array System (SABiosciences).

For each sample 10 µl of mix was pipetted into each well. RT-PCR was performed in a CFX384 Real-Time System (Bio-rad).

Results were analyzed using β-actin as reference and fold changes were determined in relation to the control sample. Genes of interest were considered based on total fold change, reproducibility of result and possible role in our *in vivo* assays.

Validation of the gene array results was done for each gene of interest (bai1, hey1, thbsp1, timp3). An RT-PCR was done for 8 different controls and 8 different catalase transfected cell cultures, using 18S as reference and the following primers:

Gene	Primer ID	Sequence 5'→3'
Bai1	mBai1F	GGATGTGGATCTGGCCTGTAG
	mBai1R	TCGCTTGAAGGTACCTGTGATAGT
Hey1	mHey1F	GCGCACGCCCTTGCT
	mHey1R	GCCAGGCATTCCCGAAAT
Thbs1	mThbs1F	CTGCAAAGGAATGCATGCTAAT
	mThbs1R	CCACGGCTGCCATGGT
Timp3	mTIMP3F	CCAACATCTTTTCCATCTTAATCCA
	mTIMP3R	CCATGTAAAAGGGAGGTGATTACC

Table 8: Primers used for RT-PCR confirmation of gene array results for genes bai1, hey1, thbsp1 and timp3.

cDNAs were diluted 1:3 and a calibration curve using further dilutions between 1:10 and 1:10000 was done for each gene. A control without cDNA template was also used for each gene. The following components were added:

Components	Volume (µl)
Sybr Green	7,5
Forward primer (10 µM)	0,45
Reverse primer (10 µM)	0,45
ddH_2O	5,6
Total volume	14

Table 9: Reagents used for RT-PCR confirmation of gene array results for genes bai1, hey1, thbsp1 and timp3.

This mix and 1 µl of diluted cDNA were added to each well and RT-PCR was performed in a CFX384 Real-Time System (Bio-rad).

Results were analyzed using 18S as reference and fold changes were determined in relation to the control samples.

7. Immunocytochemistry for Bai1, Timp3, Thbs1 and catalase

In this technique, antibodies specific to proteins of interest are used to observe differences in protein expression and cellular localization.

Specifically, we used antibodies for the proteins with significant fold-changes in expression as detected by RT-PCR, to visualize these changes within the cells as well as catalase antibody to observe catalase overexpression

Antibodies used were BAI1 antibody (NBP1-00723), TIMP3 antibody (NB110-61002), Thrombospondin1 A4.1 (NB600-554) all from Novus Biologicals and catalase (H-300) from Santa Cruz Biotech.

Cells were seeded over coverslips and the following conditions were tested:

a) 4T1 cell cultures transfected with catalase or transfected with control plasmid, 24 hours after transfection.

b) 4T1 cell cultures grown for 24 hours in conditioned media from cultures transfected with catalase or transfected with control.

c) 4T1 cell cultures grown for 24 hours in media containing extracellular catalase in the following amounts: 10U/ml, 50U/ml, 100U/ml and 250U/ml

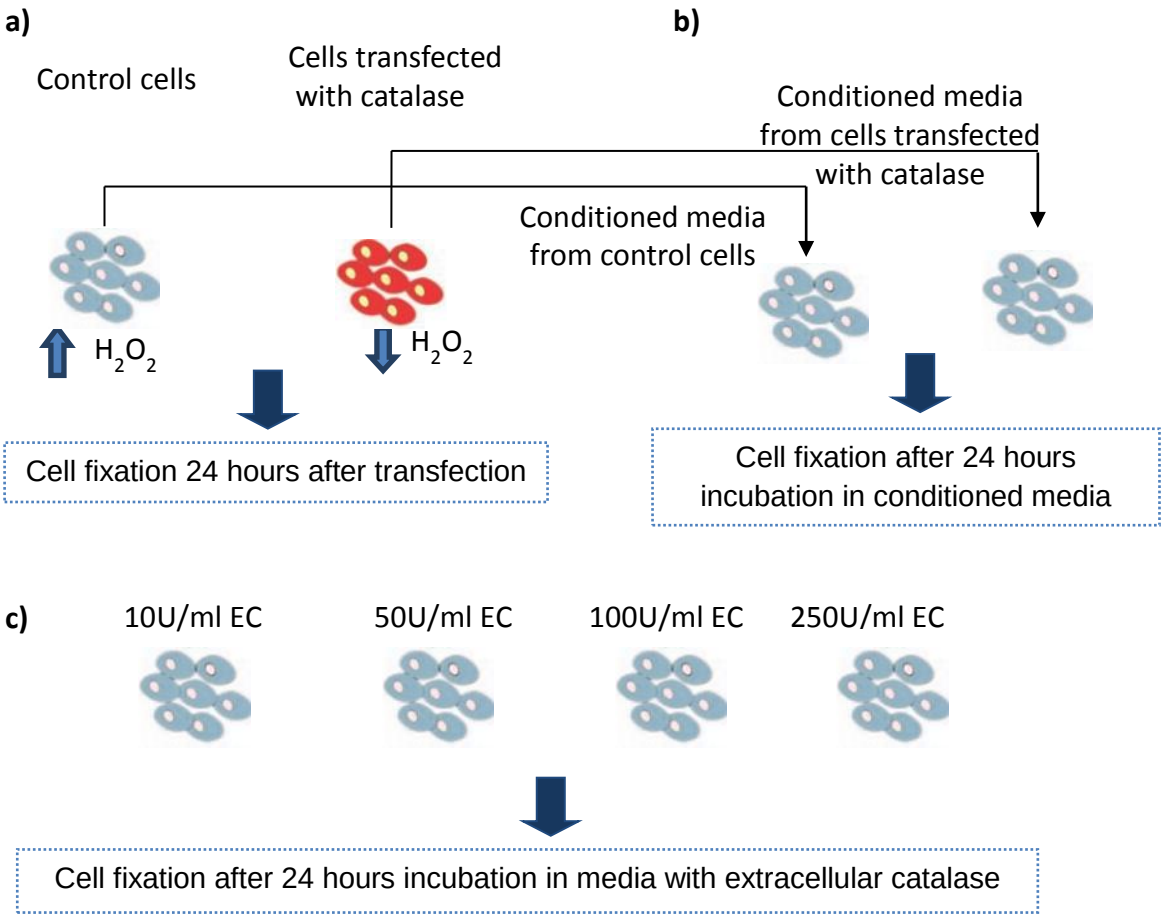

Fig 10: Experimental design for immunofluorescence studies. Experiment a) analyses differences in control vs catalase transfected cells, experiment b) analyses differences in cells incubated with conditioned media from experiment a) and experiment c) analyzes the effect of extracellular catalase on the expression of target proteins.

Cells were washed 3 times with PBS, fixed in 4% PFA (paraformaldehyde) for 30 minutes at room temperature and again washed 3 times with PBS. For TIMP3 and Thrombospondin1, which have a cytoplasmic localization, cells were permeabilized by incubating in a PBS 0,5% Triton solution for 20 minutes at room temperature.

Blocking was done with PBS 10% FBS for approximately 1 hour at room temperature after which the appropriate primary antibody was added after being diluted 1:100 in

PBS 10% FBS. These preparations were left at 4ºC O/N in a humid environment to prevent the cells drying out.

Cells were again washed 3 times for 5 minutes each with PBS and then incubated with the appropriate secondary antibody conjugated with a fluorescent dye (anti-rabbit or anti-mouse Alexa Fluor® 488 (Invitrogen)) for 2 hours at room temperature in the dark.

Cells were again washed with PBS and stained with DAPI as described in section 2.3.

The coverslips were mounted on a lamella with mowiol® (Sigma-Aldrich) and cells were observed using an Olympus BX60 microscope with 40x amplification. Excitation wavelengths of 530-550 were used for mCherry, 470-490 for Alexa Fluor 488 and 330-385 for DAPI.

For quantification of percentage of positive cells, random fields were photographed and those with 3 or more positive cells were chosen. The number of positive cells/total of cells was determined for each field and the average and standard deviation for each experiment was calculated using Excel as was p-value for each condition.

8. *IN SITU* HYBRIDIZATION ANALYSIS OF NOTCH PATHWAY GENE EXPRESSION

We used digoxigenin-labelled RNA probes with complementary sequences to several genes involved in the notch pathway to perform *in situ* hybridization followed by immunocytochemistry of catalase in order to compare gene expression and catalase expression.

The plasmid encoding the probe for Hey2 was a gift from Dr. A. Duarte and the prepared probes for Hey1, Dll1, Dll4, Jagged1, Notch1, Notch3, Hes1, Hes5 and Hes6 were a gift from Dr. D. Henriques (IMM, Lisbon).

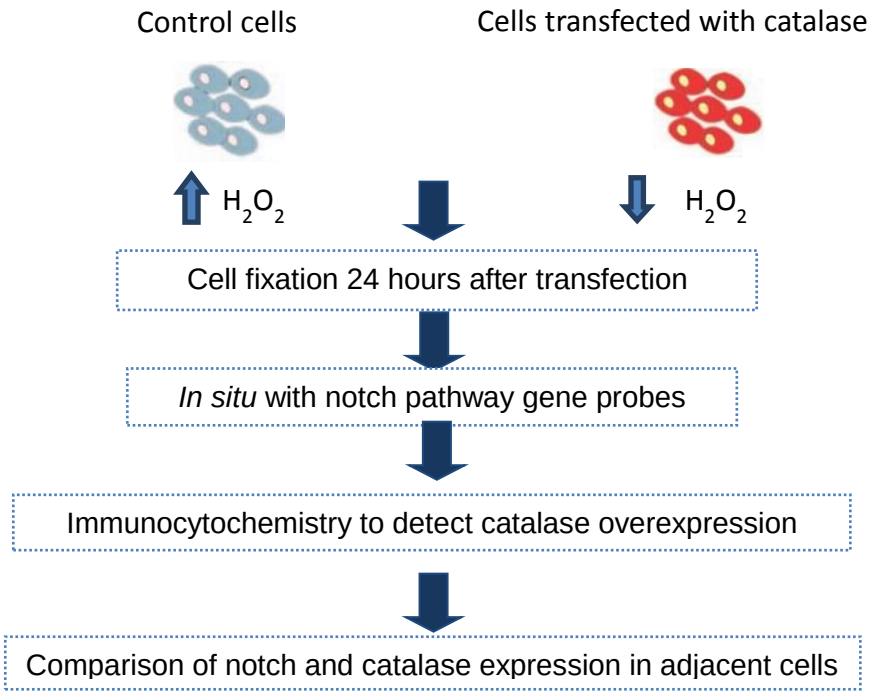

Fig. 11: Experimental design for *in situ* analysis of notch pathway gene transcripts in control and catalase transfected cells.

8.1 RNA probe preparation

The linearized plasmid was quantified using Nanodrop 1000 and diluted to 1µg/µl. The RNA probe was synthesized using the Riboprobe® in vitro transcription system (Promega) with the following quantities:

Components	Volume (µl)
Transcription buffer (5x)	4
DTT (100 mM)	2
rATP, rGTP, rCTP and DIG-11-UTP (2.5mM each) mix	4
RNAsin	1
RNA polymerase	1
Plasmid DNA	1
ddH_2O, nuclease-free	7
Total volume	20

Table 10: Reagents for synthesis of digoxigenin-labelled RNA probe

The mixture was incubated at 37ºC for 1 hour. After synthesis, DNA was removed by adding 1 µl DNAse (Thermoscientific) and 1µl RNAsin and incubating at 37ºC for another 15 minutes.

The solution was diluted to 100 µl and the RNA was precipitated with 10 µl of LiCl 4M and 300 µl of ethanol and left at -20ºC overnight. The RNA was recovered by centrifugation at 16000g for 30 minutes at 4ºC followed by washing with 75% ethanol and resuspended in TE.

RNA integrity was confirmed by running a sample in a 1% agarose gel.

8.2 *In situ* hybridization

For in situ analysis cells were transfected as described before in 24-well plates. 24 hours after transfection, media was removed and cells were washed twice with a PBS/EGTA solution with pH 7,5 and then fixated with formaldehyde 4% in PBS/EGTA for 2 hours at room temperature. After fixation cells were washed for 5 minutes in PBT twice and next dehydrated 5 minutes in 50% methanol/PBT and 5 minutes in 100% methanol twice. Fixated cells were stored in methanol at -20ºC for up to 2 weeks.

Cells were rehydrated by incubating for 5 minutes in each of the following solutions: 75%, 50% and 25% methanol/PBT and then washed twice for 5 minutes in PBT.

Cells were washed with a solution of PBT/hybridization mix (1:1) followed by rinsing several times with hybridization mix and finally incubating the cells in hybridization mix at 70ºC for 2hours.

Each probe was diluted in hybridization mix to a final concentration of 0,5 mg/ml, pre-heated to 70ºC and cells were left in this solution overnight at 70ºC. After rinsing with mix hybridization, cells were washed with hybridization mix twice for 40 minutes followed by 30 minutes with a hybridization mix/MABT (1:1) solution at 70ºC with gentle agitation.

Cells were washed a further 3 times for 30 minutes with MABT (maleic acid buffer containing Tween 20) at room temperature followed by blocking in a 2% blocking reagent (Roche), 20% sheep serum in MABT solution for 2 hours. Cells were then incubated with alkaline phosphatase conjugated anti-digoxigenin antibody (Roche) diluted 1:2000 in the same solution overnight at 4ºC.

Cells were washed 4 times for 1 hour in MABT followed by 2 washes of 10 minutes with freshly prepared NTMT and then incubated with the substrates NBT/BCIP (Promega) until color detection after which the reaction was stopped by washing with PBT. Catalase overexpression was detected by immunofluorescence as described in section 7.

9. Cloning of the pBRTol-2-flk1-KalTA4ERT2 plasmid

In order to obtain a transgenic Zebrafish overexpressing catalase in endothelial cells upon external stimulation tg(*flk1*:KalTA4), a combination of the Gal4ff-UAS-system, estrogen receptor sensitive to tamoxifen and endothelial specific promoter flk1 were cloned into a Tol-2 transposon system.

In this system, a plasmid containing a Tol-2 sequence (Urasaki, Morvan et al. 2006) and a Gal4 sequence optimized for use in Zebrafish, named KalTA4 (Distel, Wullimann et al. 2009), with the sequence for the estrogen receptor ERT2 downstream and preceded by the flk1 promoter sequence acts as the activator construct.

A similar plasmid containing a Tol-2 sequence, the UAS to which Kalt4 binds followed by the human catalase and mCherry genes is the effector construct and will be used to create the transgenic tg(UAS:catalase). By crossing these 2 lines, the transgenic tg(*flk1*:KalTA4; UAS:catalase) will be obtained where, upon tamoxifen addition, KalTA4 activator transactivates UAS dependent genes, resulting in this case in both catalase and mCherry protein production.

Because KalTA4 expression is promoted by flk1, the activator is present only in endothelium, giving catalase overexpression cell type specificity.

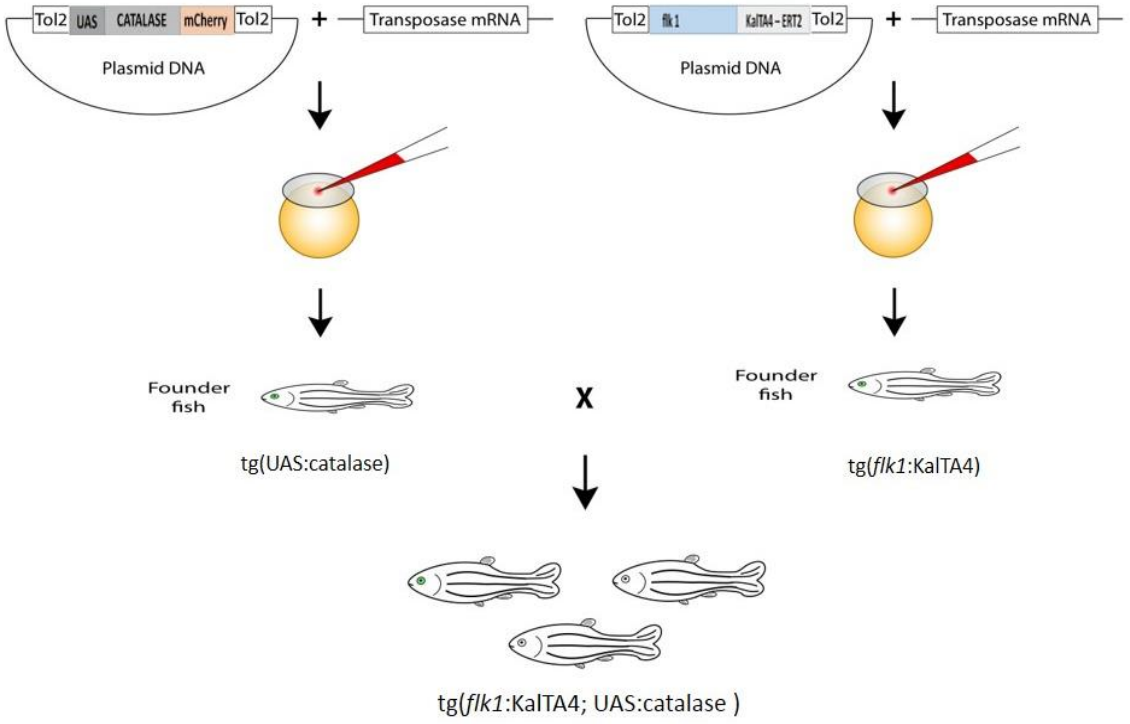

Fig. 12: Experimental design for creating a Zebrafish transgenic to express catalase in endothelial cells in a time-controlled manner. The tg(*flk1*:KalTA4) line will be crossed with tg(UAS:catalase) and in presence of tamoxifen tg(*flk1*:KalTA4; UAS:catalase) will express catalase in endothelium.

Additionally, the KalTA4 activator transcription is tamoxifen inducible because it is fused to an estrogen receptor (ERT2) sequence. The protein Hsp90 binds to ERT2 in the cytoplasm, inactivating it. When tamoxifen, an estrogen analog, is added, it binds to ERT2 causing the translocation of the entire sequence to the nucleus where transcription factors bind to the flk1 promoter leading to KalTA4 transcription.

KalTA4 will then bind to the UAS sequence leading to transcription of both catalase and mCherry in endothelial cells in a time-controlled and site-specific manner (Hans, Kaslin et al. 2009).

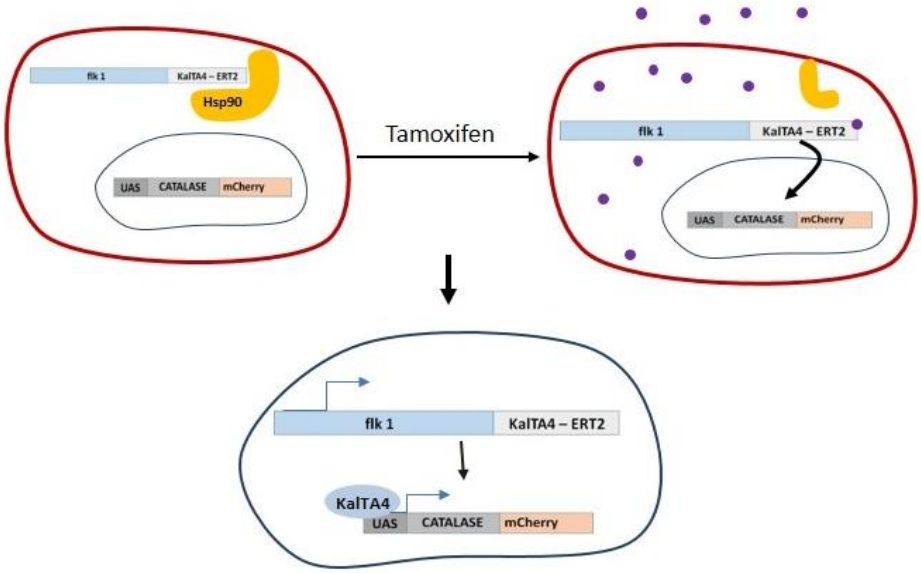

Fig. 13: Mechanism of tamoxifen dependent catalase overexpression in Zebrafish endothelial cells. Catalase expression in endothelial cells using the KalTA4 system is dependent upon addition of tamoxifen to Zebrafish embryo media which leads to translocation of the flk1 promoter to the nucleus and subsequent translation of KalTA4 which then binds to the UAS sequence activating transcription of catalase and mCherry.

Our strategy for cloning the pBRTol-2-flk1-KalTA4ERT2 plasmid was to obtain the flk1 fragment by digesting pCRIITopo-flk1 with the restriction enzymes *Xho*I and *Eco*RV, amplify the KalTA4-ERT2 sequence on pCS2 using the sp6 and T3 universal primers followed by a *Not*I digestion and do a triple ligation with these fragments and the pBR-Tol2 vector digested with *Xho*I and *Not*I (Fig. 15)

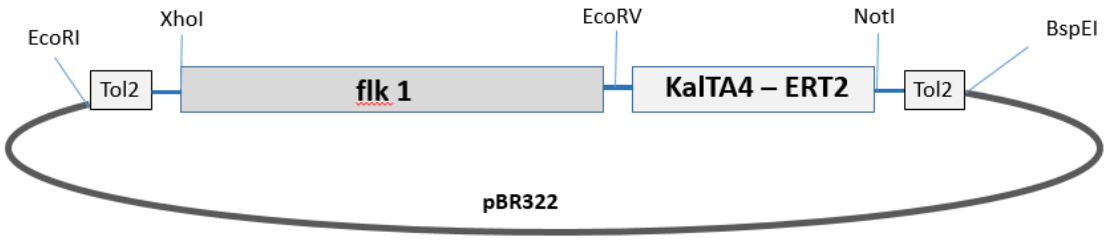

Fig.14: Map of plasmid pBRTol2-flk1-KalTA4-ERT2. Sites denoting the restriction enzymes used for cloning are indicated.

The fragments obtained were purified, the KalTA4-ERT2 fragment was phosphorylated at its 3' blunt end and the pBRTol2 vector was dephosphorylated after digestion to minimize relegation and false positive transformants.

The detailed cloning strategy is presented schematically in Fig. 15 below.

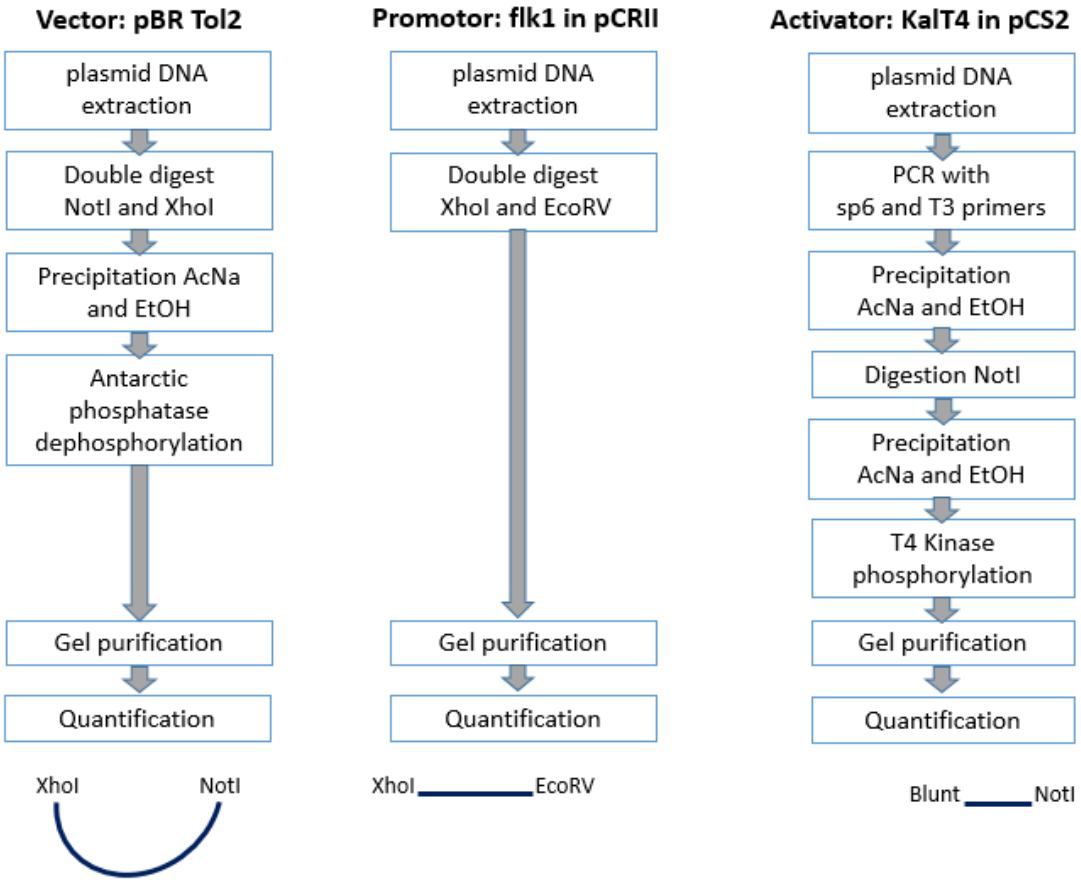

Fig. 15: Experimental design for cloning of the pBRTol2-flk1-KalTA4-ERT2 plasmid.

9.1 *E. coli* culture

The *E. coli* (DH5t strain) were grown in LB media supplemented with 100 mg/ml ampicillin for the cells containing the pCRIItopo or the pCS2 plasmid and 20 mg/ml for the cells containing the pBR- Tol2 plasmid, which is a low-copy number plasmid, O/N at 37ºC with 200 rpm agitation.

9.2 Plasmid DNA extraction

Plasmid DNA was extracted using the Wizard® Plus SV Miniprep kit from Promega following manufacturers' instructions. Briefly, 3 ml of bacterial culture were centrifuged at 16000g for 5 minutes. The supernatant was discarded and the cells resuspended by vortexing in 250 µl of resuspension solution. The same volume of lysis solution was added and the suspension was gently mixed after which 10 µl of alkaline protease solution was mixed in by inversion and left to incubate for 5 minutes at room temperature. The reaction was stopped by adding 350 µl of neutralization solution and

bacterial debris collected by centrifugation at 16000g for 10 minutes. The resulting lysate was poured into a spin column which was centrifuged at 16000g for 1 minute. The column was then washed twice with 750 µl and 250 µl of wash solution followed by similar centrifugation steps. The spin column was then transferred to a sterile tube and 100 µl and 50 µl, for high copy number and for low copy number plasmids, respectively, were added followed by centrifugation at 16000g for 1 minute to collect the plasmid DNA.

The plasmidic DNA concentration was measured using the Nanodrop 1000.

9.3 DNA fragment amplification by PCR

The KalTA4-ERT2 fragment was amplified using the sp6 and T3 primers in the pCS2 plasmid with the following sequences:

Name	5'→3' sequence
SP6	AAGCTTGATTTAGGTGACACTATAG
T3	CAATTAACCCTCACTAAAGGGA

Table 11: Sequence of primers sp6 and T3 used to amplify the KalTA4-ERT2 fragment.

For the PCR the following reagents were used:

Reagent	Quantity
Phusion buffer (5x) Thermo Scientific	4 µl
dNTPs (10 mM)	0,4 µl
sp6 primer (10µM)	1 µl
T3 primer (10 µM)	1 µl
pCS2-KalTA4-ERT2 DNA (1 ng/µl)	1 µl
Phusion DNA polymerase (2U/µl) (ThermoScientific)	0,2 µl
ddH_2O, nuclease-free	To 20 µl

Table 12: Reagents used for the PCR amplification of the KalTA4-ERT2 fragment.

The PCR program (in a PTC-100 thermocycler) used was:

Denaturation	98ºC	30 sec
Denaturation	98ºC	15 sec
Annealing	60ºC	1 min 30 sec
Extension	72ºC	1 min 30 sec
Extension	72ºC	10 min

X 29

The PCR product was visualized in 1% agarose gel.

9.4 DNA precipitation

The PCR product and digestion products solution in intermediate steps were precipitated to remove salts and proteins before further steps were carried out. This was done by adding 1/10 of the solution volume of sodium acetate 3M and twice the solution volume of ethanol 96% and putting the mixture at -20ºC O/N. The following day, tubes were centrifuged at 16000g, 4ºC for 30 minutes and the supernatant removed. 500 µl of ethanol at 70% was added followed by centrifugation at 16000g, 4ºC for 10 minutes. The supernatant was thoroughly removed, the pellet left to air dry for a few minutes and then resuspended in an appropriate volume of MQ water.

9.5 DNA fragment restriction enzyme digestions

The double digestion to obtain the flk1 fragment was performed by adding the following reagents:

Reagent	Quantity
Buffer 3 (10x) New England Biolabs	10 µl
BSA (100x) New England Biolabs	1 µl
*Xho*I (10 U/µl) Fermentas	4 µl
*Eco*RV (20 U/µl) Fermentas	2 µl
pCS2-flk1 DNA (1850 ng/µl)	2,16 µl (4 µg)
ddH_2O, nuclease-free	To 100 µl

Table 13: Reagents used for the digestion of the pCRTopo plasmid in restriction sites flanking the flk1 promoter.

The digestion mix was incubated at 37ºC O/N.

For the double digestion of the pBRTol-2 vector the following reagents were added:

Reagent	Quantity
Buffer 3 (10x) New England Biolabs	10 µl
BSA (100x) New England Biolabs	1 µl
*Xho*I (10 U/µl) Fermentas	4 µl
*Not*I (10 U/µl) New England Biolabs	4 µl
pBR Tol2 DNA (273 ng/µl)	14,6 µl (4 µg)
ddH_2O, nuclease-free	To 100 µl

Table 14: Reagents used for the digestion of the pBRTol2 plasmid vector.

The digestion mix was incubated at 37ºC O/N.

For the digestion of the PCR fragment containing KalTA4 and ERT2 the following reagents were added:

Reagent	Quantity
Buffer 3 (10x) New England Biolabs	10 µl
BSA (100x) New England Biolabs	1 µl
*Not*I (10 U/µl) New England Biolabs	4 µl
KalTA4 PCR product (187,7 ng/µl)	21 µl (4 µg)
ddH_2O, nuclease-free	To 100 µl

Table 15: Reagents used for the digestion of the KalTA4-ERT2 fragment amplified by PCR.

The digestion mix was incubated at 37ºC O/N.

The digestion products KalTA4 and pBRTol-2 were precipitated as described above and flk1 was purified by gel.

9.6 Dephosphorylation of the pBRTol-2 vector

After precipitation, the pDNA was resuspended in 43 µl of MQ water to which 5 µl of Antarctic phosphatase buffer (10x) and 2 µl of Antarctic phosphatase (both from New England Biolabs) were added. The mix was incubated for 1 hour and 30 minutes at 37ºC.

9.7 Phosphorylation of KalTA4 fragment

After precipitation, the KalTA4 fragment resuspended in 15 µl of MQ water to which 2 µl of Buffer A (10x), 2 µl of ATP (10µM) and 1 µl of T4 kinase (10 U/µl) (Thermoscientific). The mixture was incubated at 37ºC for 30 minutes followed by 10 minutes at 75ºC to inactivate the enzyme.

9.8 DNA purification by gel extraction

DNA fragments were ran on a 1% agarose gel at 90V for approximately 30 minutes, bands of interest were excised by comparing band size with the Generuler 1 Kb DNA ladder (Thermoscientific) and purified using the Wizard® SV gel and PCR clean-up system from Promega. Briefly, the excised band was weighed and 10 µl of membrane binding solution per 10 mg of gel was added, the mixture was vortexed and incubated

at 55ºC until the gel dissolved. The mixture was then transferred to the SV minicolumn, left to incubate for 1 minute at room temperature and centrifuged at 16000g for 1 minute. The flowthrough was discarded and the column was washed twice, with 700 µl, followed by a 1 minute centrifugation at 16000g, and 500 µl of membrane wash solution followed by a 5 minute centrifugation at 16000g. The DNA was eluted by adding 30 µl of MQ water to the column, incubated for 1 minute and centrifuged at 16000g for 1 minute and stored at -20ºC.

9.9 DNA quantification

DNA fragments were quantified by running 1 µl of purified solution in a 1% agarose gel and comparing with the Generuler 1 Kb DNA ladder (Thermoscientific).

9.10 Ligation

The appropriate amounts of each fragment plus 1 µl of ligation buffer 10x (Fermentas) and 1µl of ligase (Fermentas) and MQ water to a total of 10 µl were added and incubated at 16ºC O/N.

9.11 Competent *E. coli* by the Inoue method

The DH5t *E. coli* strain was used to make competent cells for transformation (Inoue, Nojima et al. 1990). Cells were streaked in an agar-LB plate without antibiotic and incubated O/N at 37ºC. A pre-culture with 25 ml of SOB supplemented with 10 mM $MgCl_2$ and 10 mM $MgSO_4$ and inoculated with a single colony from the plate was incubated O/N at 37ºC and 250 rpm. The following day, 1 ml of pre-culture was used to inoculate 125 ml of SOB supplemented as described above and incubated at 18ºC, 250 rpm for 24-26hours.

After 24 hours incubation, O.D. of the culture was measured at 600 nm, starting at 30 minutes intervals and diminishing as O.D. increased. When O.D. reached 0,6, the culture was iced for 10 minutes, then placed in a sterile centrifuge flask and centrifuged at 2500g, 4ºC for 10 minutes and the supernatant removed. The cells were very gently resuspended in 40 ml of chilled transformation buffer and incubated on ice for another 10 minutes followed by centrifugation at 2500g, 4ºC for 10 minutes. The

supernatant was removed and the cells resuspended in 10 ml of chilled transformation buffer. DMSO (dimethyl sulfoxide) to a final concentration of 7% was added and aliquots of 100 µl were made and immediately frozen in liquid nitrogen. Cell aliquots were stored at -80ºC.

9.12 Transformation

An aliquot of competent bacteria was slowly thawed and ligation mix was added to the cells, gently mixed and placed on ice for 20 minutes. A control with 1 µl of digested and dephosphorylated vector plasmid DNA was used following the same procedure. The mixtures were then placed in a water bath at 42ºC for 90 seconds and immediately put on ice for another 5 minutes after which 900µl of LB media were added to each tube. The cultures were incubated for 1 hour at 37ºC, 200 rpm. After incubation, cells were centrifuged at 5000g for 2 minutes and 900µl of supernatant were removed. Cells were resuspended in the leftover media and then spread in an LB-agar containing 20 mg/ml of ampicillin plate and incubated at 37ºC O/N.

9.13 Testing for the pBRTol2-flk1-KalTA4-ERT2 plasmid in transformants

Single colonies were picked from the transformants plate and grown in 5 ml LB with 20 mg/ml ampicillin at 37ºC, 250 rpm O/N. Cultures were centrifuged at 15000g for 10 minutes and the supernatant discarded. Approximately 5 µl of pellet were added to 20 µl of cracking buffer and incubated at 55ºC for 30 minutes followed by vortexing for 1 minute. DNA was visualized in a 1% agarose gel and transformants with bands over 10000 bp were selected for further testing. Plasmidic DNA was extracted from the remaining pellet using the Wizard® Plus SV Miniprep kit as described previously and different restriction enzyme digestions were used to check for the presence of the relevant fragments.

RESULTS

Previous results obtained in our laboratory (Rodrigues, G., Ms Thesis, 2011) have shown that lower levels of H_2O_2 in tumor cells, due to transient catalase overexpression, affect *in vivo* angiogenesis.

The present work focused in identifying the molecular mechanisms involved in the crosstalk between tumor cells and endothelial cells that may be responsible for the observed phenotype.

1. CATALASE OVEREXPRESSION IN 4T1 CELLS

In order to identify tumor cells with catalase overexpression, we created a plasmid that co-expressed a reporter protein, mCherry, as well as catalase in the same cell. We have also optimized the transfection procedure for 4T1 cell line.

1.1. Cloning catalase in pCIC-IRES-mCherry-NLS

A construct containing catalase and the fluorescent protein mCherry was made using the pCIC-IRES-mCherry-NLS plasmid (fig. 16).

This vector allows the independent expression of catalase and mcherry in the same cell without the production of a fusion protein. This plasmid will be referred to as pCIC-Cat (pCIC-Catalase-IRES-mCherryNLS).

The vector contains mCherry with an NLS (nuclear localization sequence) which directs the fluorescent protein towards the nucleus. The presence of an IRES sequence (independent ribosome entry site) downstream of the gene of interest enhances mCherry translation to ensure that all cells expressing catalase will also express the reporter gene.

In the subsequent experiments the plasmid containing only the mCherry sequence, here referred to as pCIC, was used as control.

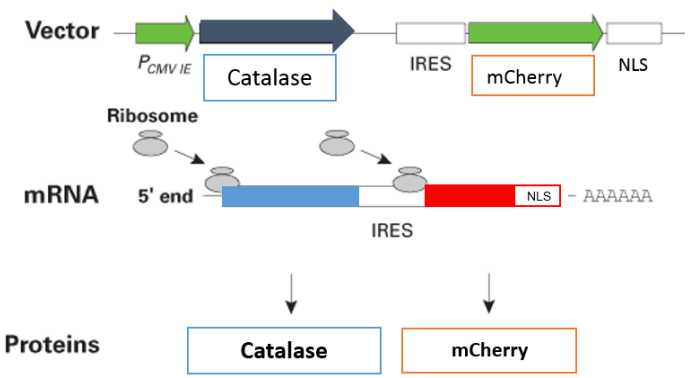

Fig. 16: Construction of pCIC-Cat plasmid for catalase overexpression. pCIC-Cat allows the independent overexpression of catalase and mCherry (IRES: independent ribosome entry site, NLS: nuclear localization sequence).

1.2 Optimization of 4T1 cell transfection

Due to the low transfection efficiency of the previously developed method (7,07 ± 2,53%) it was necessary further optimization.

The transfection reagents Lipofectamine® 2000 (Invitrogen) and Fugene® 6 (Promega) were tested using the plasmid pCIC and an initial screening of best cell density and DNA/liposome ratio was performed by comparing variations in mCherry fluorescence using a microplate reader (fig. 17)

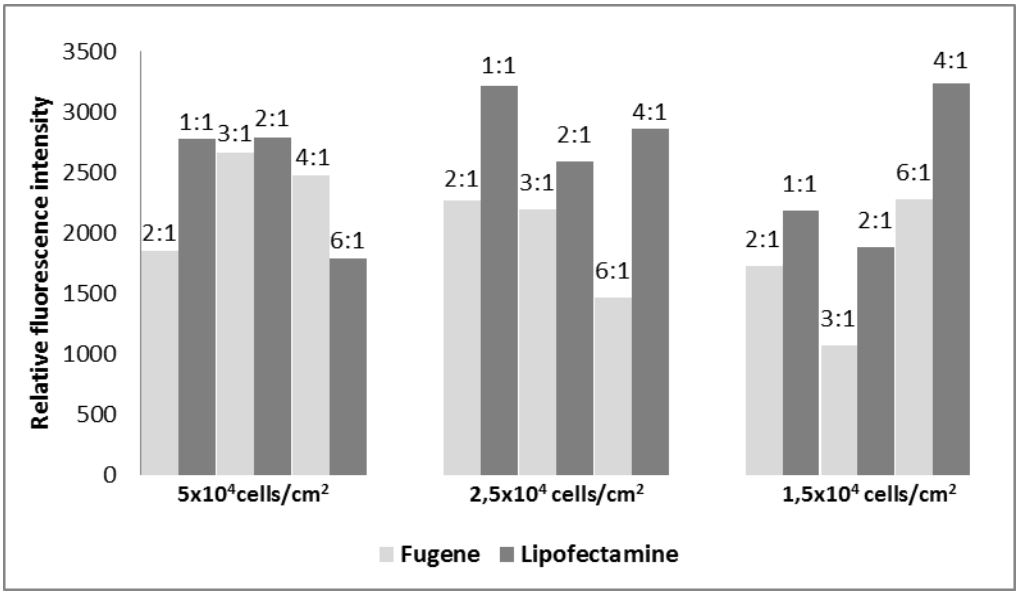

Fig. 17: Relative fluorescence obtained with different transfection protocols using Fugene6 and Lipofectamine 2000 reagents. Fluorescence at 610nm was measured 24 hrs after transfection with pCIC-Cat. Data labels represent the transfection reagent to DNA ratio in µl/µg.

The best transfection conditions were further tested with cell transfection being determined by cell counting using fluorescence microscopy and FACS.

The best condition used lipofectamine as transfection reagent in a 1:1 ratio of (µl lipofectamine):(µg DNA) and cells seeded at $2,5x10^4$ cells/cm^2 16 hours before transfection and yielded a transfection efficiency of 16,7 ± 2,78% in contrast with 7% initially obtained.

1.3 Catalase expression and activity in 4T1 cells transfected with pCIC-Cat

To confirm catalase expression in mCherry positive cells we have performed immunofluorescence.

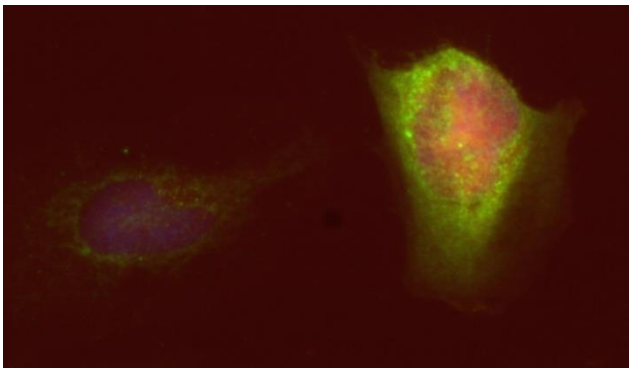

Fig. 18: Catalase expression in 4T1 cells transfected with pCIC-Cat. Immunocytochemistry of 4T1 cells transfected with mCherry and catalase. mCherry (red) positive cells present overexpression of catalase (green) when compared with non-transfected cells (stained blue using DAPI).

The cells transfected with the pCIC-Cat plasmid (referred to as CatO cells) presented an increase in catalase expression compared with mcherry negative cells (fig.18).

Catalase is a multimeric protein containing four subunits whose assembly is necessary for enzymatic activity. To verify whether the catalase overexpressed was functional in transfected cells, catalase activity was measured by a zimography assay. This was achieved by protein separation in native gel, followed by observation of hydrogen peroxide consumption using a chromogenic product (Materials and methods section 4).

The protein extract used for this assay was obtained at 8, 16 and 24 hours after transfection, to determine the best end time for further experiments. The highest increase in catalase activity was achieved 24 hours post-transfection and this timepoint was chosen for subsequent experiments.

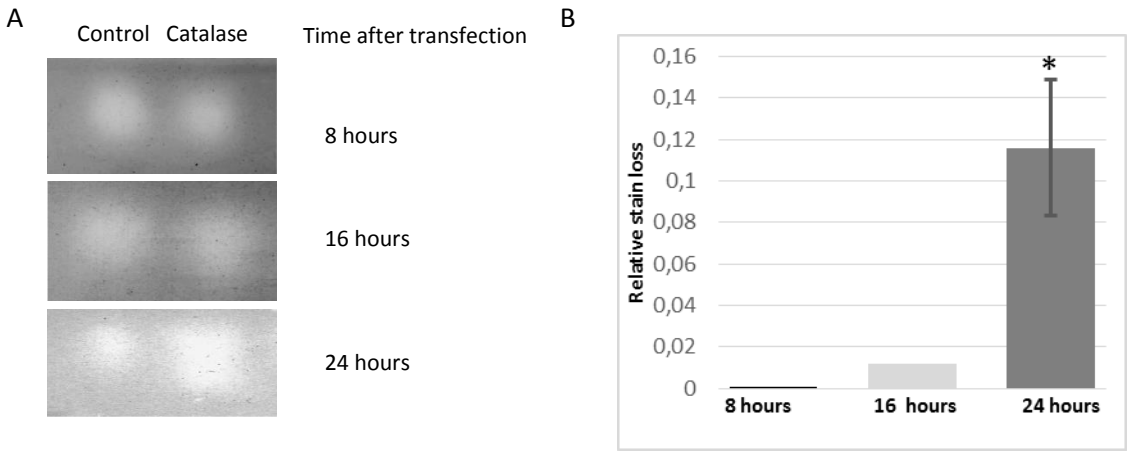

Fig. 19: Catalase activity in 4T1 cells transfected with pCIC-Cat at different timepoints. (A)Hydrogen peroxide presence was detected by gel staining. Catalase activity corresponds to higher level of stain fading. (B). catalase activity quantification ($P<0,05$, n=3).

2. HIF1α expression in 4T1 cells *in vitro*

In hypoxic conditions (5-10% oxygen), HIF1α is the key regulator of angiogenesis and is known to be regulated by H_2O_2.

In this work we were interested in finding H_2O_2 targets that are independent of HIF1α regulation and so we determined HIF 1α expression by western blot. We compared the expression of HIF 1α in protein extracts from 4T1 in normoxia and in hypoxia (5% oxygen) and also confirmed the effect of catalase overexpression on HIF 1α in the 4T1 cell line.

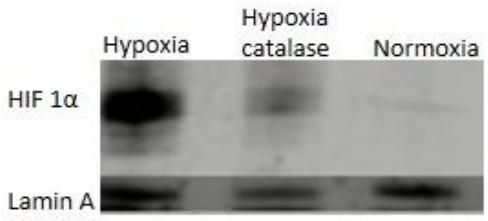

Fig. 20: Western blot of HIF 1α. HIF 1α expression in hypoxia (5% O_2) in 4T1 control cells, in hypoxia in 4T1 CatO cells and in normoxia in 4T1 control cells.

We observed that, in normoxia, HIF 1α expression is too low to detect. In addition, overexpression of catalase is enough to decrease the overall amount of HIF1α when compared to control cells, as previously described (Brunelle, Bell et al. 2005).

The negligible effect of HIF1 in tumor cells cultured in normoxia conditions (21% oxygen) allows for the study of other factors controlled by H_2O_2, which are independent of HIF1α regulation.

3. H_2O_2-dependent regulation of gene expression in the 4T1 cell line

In order to test whether the reduction in H_2O_2 cellular levels affected the expression of genes known to be involved in the angiogenic process, we used a PCR-Array focused on pro and anti-angiogenic genes.

Figure 21 presents the gene expression ratio between CatO cells and control cells.

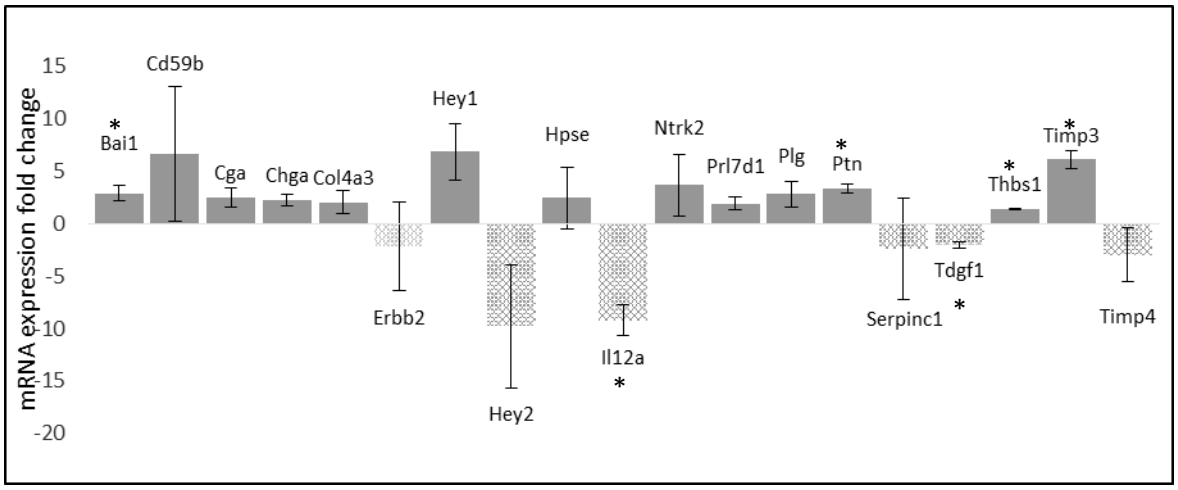

Fig. 21: Angiogenesis related genes expressed in CatO 4T1 cells. The genes with an average mRNA expression change > 2 fold from 3 independent samples transfected with catalase vs control cell cultures are represented.

The function of genes present in Figure 21 are is described in table 16 in supplementary materials.

Of note, several overexpressed genes, namely brain-specific angiogenesis inhibitor 1, chromogranin A, Collagen, type IV, alpha 3 and plasminogen are precursors to smaller molecules that act as angiogenesis inhibitors after cleavage and can thus contribute to the phenotype observed *in vivo.* From these, we choose to analyze the role of brain-specific

angiogenesis inhibitor 1 (Bai1), thrombospondin 1 (Thbs1) and tissue inhibitor of metalloproteinase 3 (Timp3) as they have antiangiogenic properties and were significantly upregulated in CatO cells. In this first analysis, we excluded Ptn since it mainly expressed in brain tissue and Il12a that functions as antiangiogenic and was found to be downregulated. Although Hey1 and Hey2 expression was not significantly different between CatO cells and control cells, we decided to analyze the components of notch signaling pathway since they have a central role in the regulation of vessel formation and branching.

In order to validate some of the results obtained in the gene analysis, we performed an RT-PCR using control and catalase transfected 4T1 cells.

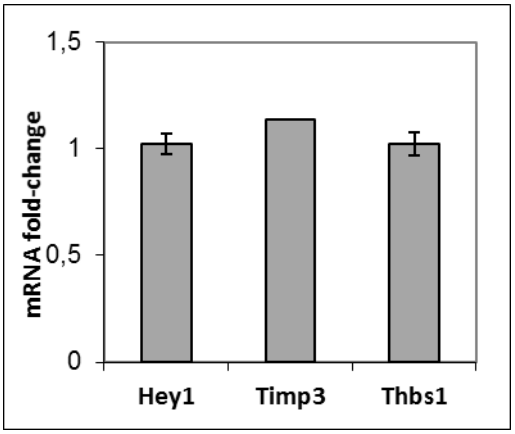

Fig. 22: Quantification of the expression of angiogenesis related genes by RT-PCR in catO cells. RT-PCR was performed using sybergreen for 3 independent experiments.

We were not able to confirm the PCR-array results since the expression of Hey1, Timp3 and Thbs1 did not present any difference between controls and CatO cells. These results might be due to low efficiency of transfection. Therefore, we decided to perform immunofluorescence and *in situ* hybridization to analyze the effect of H_2O_2 decreased levels in the regulation of gene expression.

3.1 Regulation of Notch signaling components by H_2O_2

Because it was observed, *in vivo,* that overexpression of catalase in tumor cells led to less sprouting in the angiogenic process when compared to controls (Rodrigues, G., master thesis 2011), we analyzed the expression of Notch signaling components. Using *in situ*

hybridization in cell cultures transfected with control and catalase plasmid, we analyzed the expression of notch ligands Dll1, Dll4 and Jagged1, notch receptors, Notch 1 and Notch3 and the downstream targets Hey1, Hey2, Hes1, Hes4, Hes5 and Hes6.

Of these, mRNA was only detected for Dll4, Notch3, Jagged1 and Hes1 (fig. 22).

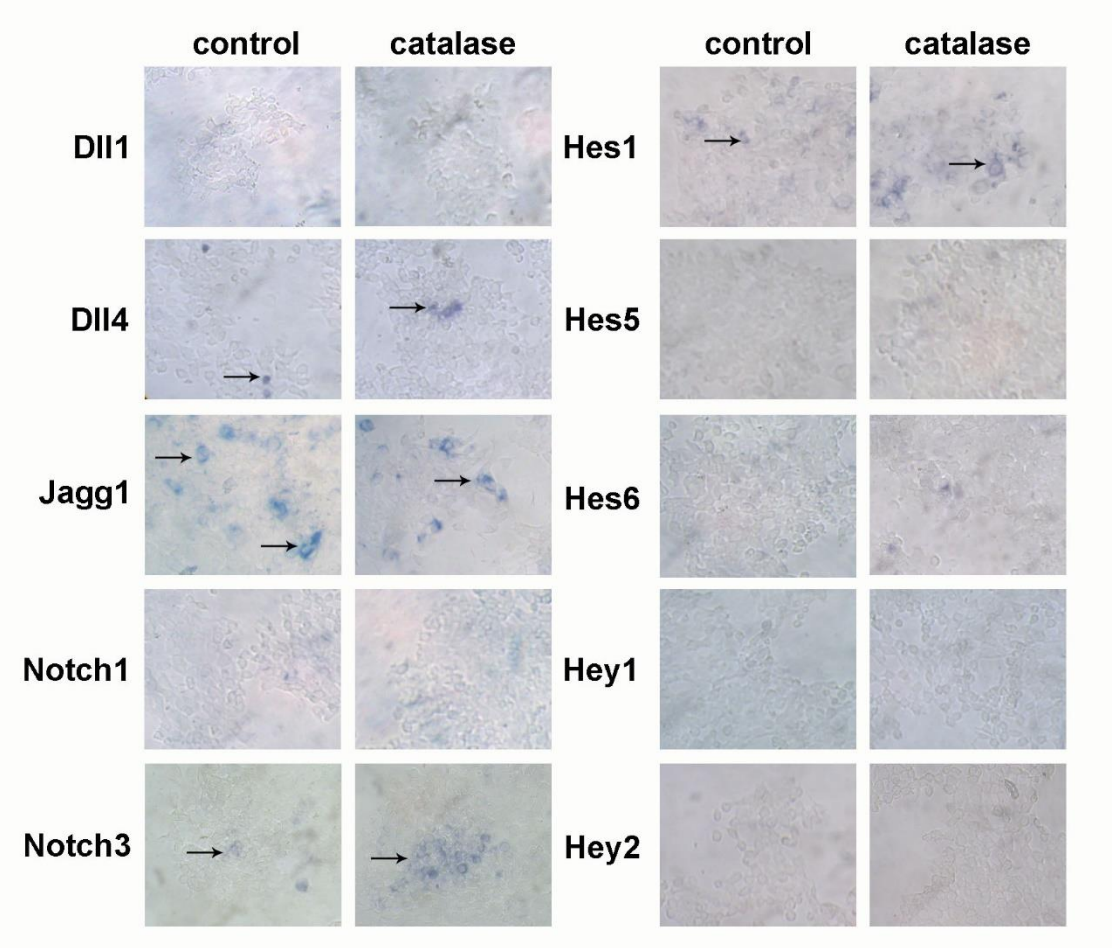

Fig. 23: I*n situ* hybridization showing expression of ligands, receptors and effectors of the notch signaling pathway in 4T1 cell cultures. mRNA in control and CatO cells was detected for Dll4, Jagg1, Notch3 and Hes1. Arrows indicate positive cells.

To determine whether changes observed in the expression of Dll4, Jagged1, Notch3 and Hes1 are dependent on catalase overexpression, immunolabelling of catalase was performed after *in situ* hybridization (fig. 24).

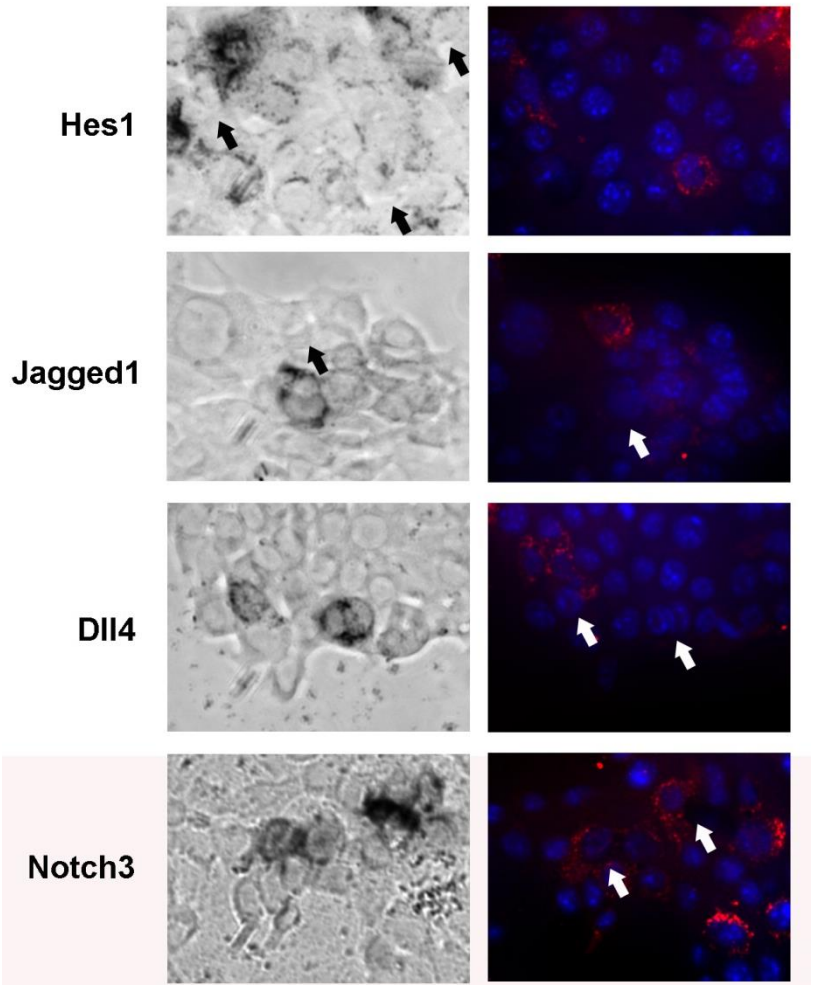

Fig. 24: Catalase overexpression and mRNA expression for Dll4, Jagged1, Notch3 and Hes1 in 4T1 cells. Catalase was detected by immunofluorescence (red) after *in situ* hybridization in 4T1 catO cell. White arrows indicate in situ hybridization positive cells; black arrows indicate catO cells.

The expression of Dll4, Notch3, Jagged1 and Hes1 occurs in cells with or without catalase overexpression. This result indicates that the overexpression of catalase is not able to regulate the expression of these genes.

Differences in the overall number of cells expressing Dll4, Notch3, Jagged1 and Hes1 in control and CatO cell cultures could not be quantified as possible non-specific hybridization made cell counting an inaccurate method to determine variations.

3.2. Regulation of protein expression of antiangiogenic factors Bai1, Timp3 and Thbs1 by catalase overexpression

To determine whether CatO cells (mCherry positive cells) presented differences in Timp3, Thbs1 and Bai1 expression levels comparing with untransfected cells (mCherry negative cells) we performed immunofluorescence assays.

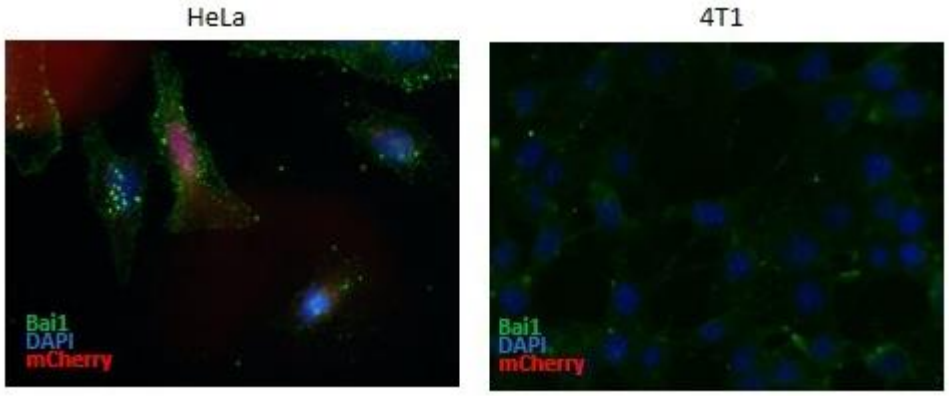

Fig. 25: Bai1 expression in HeLa and 4T1 cell cultures. Bai1 (green) was labelled with an antibody recognizing an extracellular peptide sequence and nuclei were stained with DAPI (blue).

Bai1 protein was not detected in the 4T1 cell line by immunofluorescence (fig. 25) when compared to Hela cell line.

The expression of Thbs1 occurred in both transfected and non-transfected cells and we concluded that no cell autonomous effect of catalase exists in Thbs1 expression (fig. 26).

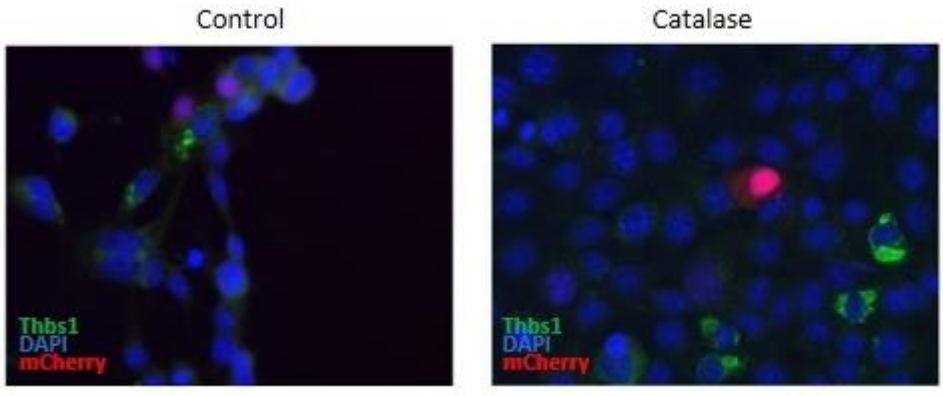

Fig. 26: Thbs 1 expression in control and catO 4T1 cells. Thbs1 (green), mCherry expression (red) indicates catalase transfected cells and nuclei were stained with DAPI (blue).

To evaluate whether an overall difference in Thbs1 expression existed between the two conditions, the number of Thbs1 positive cells in each experimental condition was counted and expressed as a percentage of the total number of cells for representative fields (fig 27).

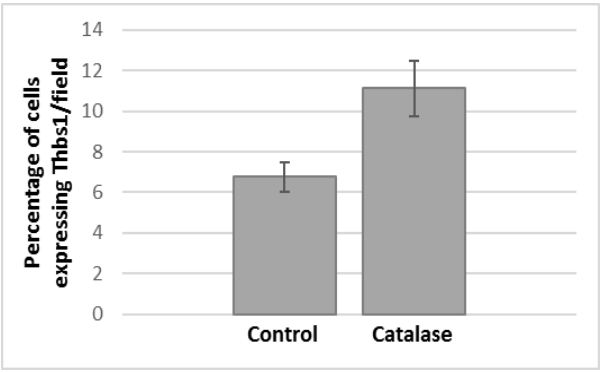

Fig. 27: Percentage of Thbs1 positive cells in control and catO 4T1 cell cultures, 24 hours after transfection (n=2) *p*=0,07.

Although not significant due to the low number of independent experiments, catalase overexpression increased the percentage of cells expressing Thbs1 from approximately 6,7% to 11,1%.

To test whether this effect was due to a decrease in H_2O_2 levels in the media we added 10U/ml, 50U/ml and 100U/ml of extracellular catalase to untransfected 4T1 cells.

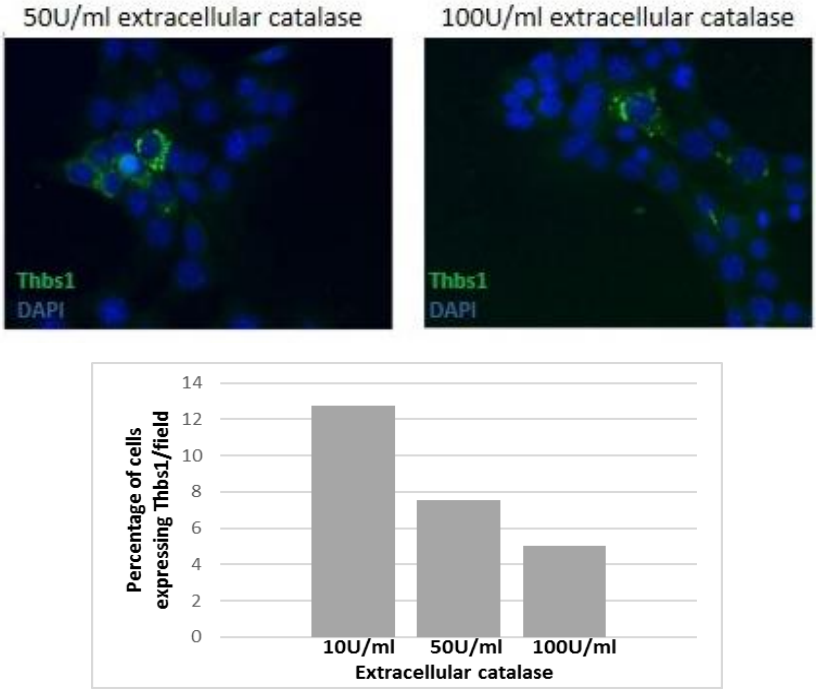

Fig. 28: Thbs1 expression in 4T1 cell cultures incubated for 24 hours with 50U/ml (right) and 100U/ml (left) of extracellular catalase. Thbs1 (green) was labelled with an antibody and nuclei were stained with DAPI (blue) (n=1).

A preliminary experiment with addition of extracellular catalase to cell media showed increase in number of cells with Thbs1 expression with 10U/ml of catalase similarly to catalase transfected cell cultures. This may mean that a decrease in extracellular H_2O_2 upregulates Thbs1 expression.

Paradoxically, increased amounts of extracellular catalase leads to a decrease in Thbs1 expression. This might indicate that an excess in catalase expression might have a secondary effect on cell promoting Thbs1 downregulation.

Further experiments are needed to confirm this result.

In order to determine whether Thbs1 expression is also regulated by a secreted factor present in the medium of catO cells we incubated untransfected cells with control or catalase transfected cell conditioned medium (CM). The number of Thbs1 positive cells in each experimental condition was counted and expressed as a percentage of the total number of cells for representative fields (fig 29).

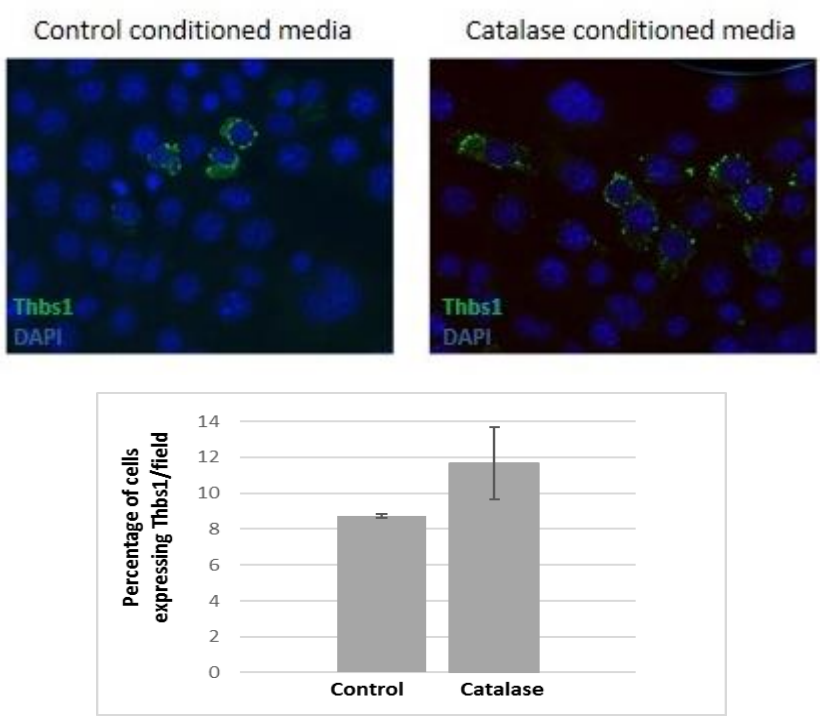

Fig. 29: Thbs1 expression in 4T1 cell cultures incubated with conditioned media from control and CatO cell cultures for 24 hours. Thbs1 expression (green) and nuclei were stained with DAPI (blue) (n=2)(*p*=0,19)

Cells treated with CM from catalase transfected cells presented higher percentage of Thbs1 positive cells (11,67%) than cells treated with CM from control cells (8,74%).

Although not significant (p=0,19), this result may indicate that CatO cells promote the production of a secreted factor that is able to regulate Thbs1 expression.

In order to determine whether the regulation of Timp3 expression was also a non-autonomous effect we tested whether extracellular regulated Timp3 expression (Fig. 30).

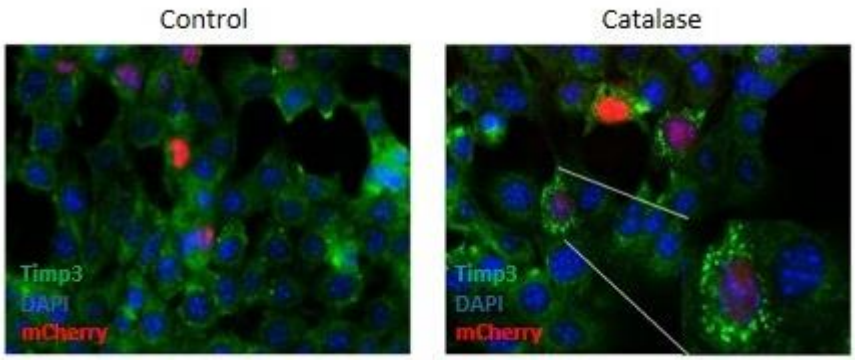

Fig. 30: Timp3 expression in control and CatO 4T1 cells. Thbs1 expression (green), mCherry expression indicates catalase transfected cells (red) and nuclei were stained with DAPI (blue).

Figure 30 shows an increase in Timp3 expression exclusively in catO cells. These results indicate that catalase regulates Timp3 expression in an autonomous manner.

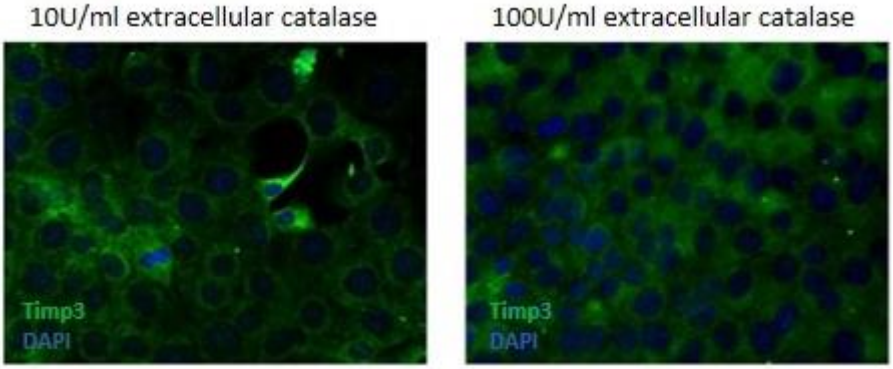

Fig 31:Timp3 expression in 4T1 cell cultures incubated for 24 hours with 10U/ml and 100U/ml of extracellular catalase. Timp3 (green) was labelled with an antibody and nuclei were stained with DAPI (blue).

As shown in figure 31 extracellular catalase did not induce the expression of Timp3 indicating that it is regulated by the expression of catalase cell autonomously.

4. Cloning of pBRTol-2-flk1-KalTA4ERT2 for production of a Zebrafish transgenic line

The pBRTol-2-flk1-KalTA4ERT2 will be used to obtain a Zebrafish transgenic line which expresses KalTA4ERT2 under the regulation of the endothelial specific flk1 promoter. KalTA4ERT2 is a fusion protein between a modified gal4 activating protein and estrogen receptor which translocates to the nucleus in presence of estrogen (Tamoxifen). This construct is cloned into a Tol-2 transposon system for genome integration in Zebrafish to produce tg(*flk1*:KalTA4) line. This line will be crossed with tg(UAS:catalase).

In presence of tamoxifen tg(*flk1*:KalTA4; UAS:catalase) will express catalase in a spatially and temporally controlled way.

The cloning strategy described in Materials and methods section 9 results in plasmid pBRTol-2 flk1-KalTA4-ERT2 with the structure below:

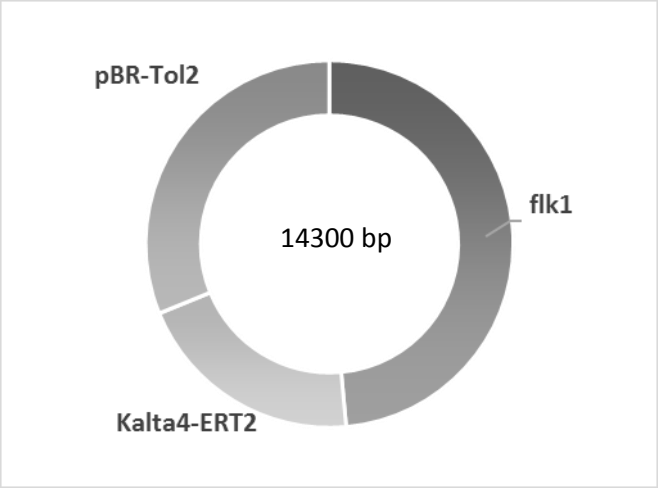

Fig. 32: Predicted structure of the pBRTol-2 flk1-KalTA4-ERT2 plasmid. The final construct will contain the vector pBRTol-2 (4500bp), the flk1 promoter (6800bp) and the KalTA4 activator and ERT2 estrogen receptor fragment (3000bp).

4.1 Screening of transformants

An initial screening was done using DNA obtained from direct bacteria lysis (cracking method) (figure 33). Transformants with larger bands were chosen for further analysis.

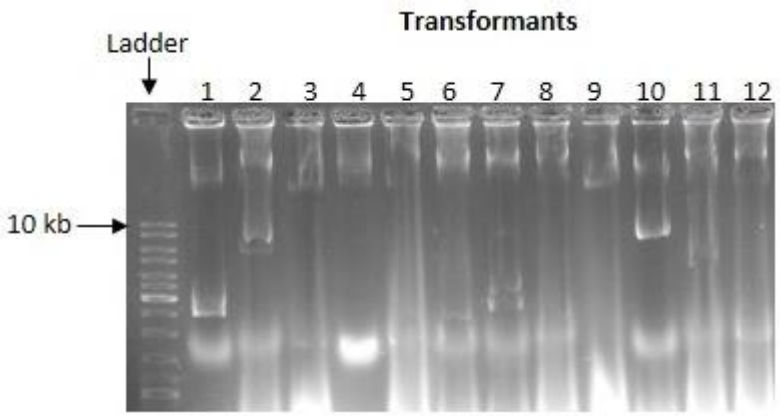

Fig. 33: Screening transformants for the pBRTol-2-flk1-KalTA4-ERT2 plasmid. DNA from 12 transformants was extracted using the cracking method and ran on a 1% agarose gel. Samples with larger sized bands (lanes 2 and 10) were chosen. Generuler 1 Kb Plus was used as size ladder.

Plasmid DNA from the chosen samples was extracted and analyzed via digestion with restriction enzymes.

4.2 Confirmation of DNA fragments in putative pBRTol-2-flk1-KalTA4-ERT2 plasmid

The plasmid was digested with *Xho*I, the same enzyme used for creating sticky ends for the pBR-Tol-2 vector and flk1 promoter and *Nco*I which has a unique site approximately 4300 bp downstream of the *Xho*I site.

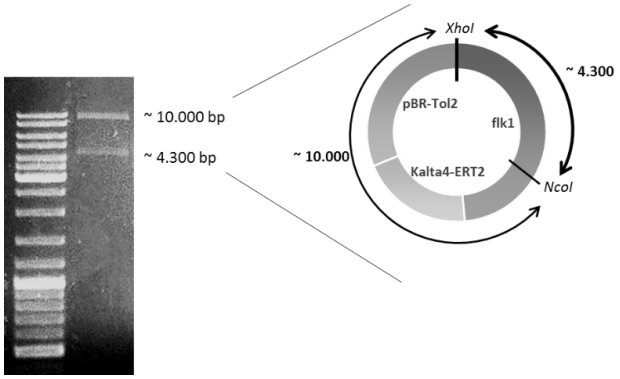

Fig. 34: Digestion of putative clone with *Xho*I and *Nco*I enzymes, yielding a fragment of flk1 promoter.

The band sizes obtained correspond to the expected ones. The plasmid will be sequenced to verify sequence accuracy prior to injection in Zebrafish oocytes.

DISCUSSION

H_2O_2 is involved in many aspects of cancer cell phenotype known to contribute to tumorigenesis, including the angiogenic process that enables tumor growth and dissemination.

Catalase overexpression in both stable transfected cell lines and transgenic models have been shown to inhibit tumor angiogenesis and slow tumor progression (Glorieux, Dejeans et al. 2011), (Goh, Enns et al. 2011). However, in these studies catalase was homogeneously overexpressed in all cells and the effect of a small subset of cells overexpressing catalase was not addressed.

Previous i*n vivo* studies using the Zebrafish xenograft model have shown that lowering levels of H_2O_2 by catalase overexpression in a small percentage of 4T1 mouse breast tumor cells decreases tumor angiogenesis and vessel invasion significantly (Rodrigues, G., Ms thesis, 2011).

The mechanisms by which this overall effect is achieved by altering only a part of tumor cells are the object of this study.

1. H_2O_2 REGULATES THE EXPRESSION OF ANGIOGENIC FACTORS

By gene array analysis, we found changes affecting the expression of Notch effectors Hey1 and Hey2 in catO cells indicating that H_2O_2-dependent regulation of angiogenesis could happen through the Notch signaling pathway. However, using *in situ* hybridization we could only verify the expression of the ligands Jagged1 and Dll4, the receptor Notch3 and the effector Hes1 in both control and catalase overexpressing cells while ligand Dll1, receptor Notch1 and effectors Hes4, Hes5, Hes6, Hey1 and Hey2 were not detected in 4T1 cells.

In the same array analysis we identified Bai1, Ptn, Tdgf, Timp3 and Thbs1 as significantly overexpressed in catO cells. Of these we chose to study Bai1, Timp3 and Thbs1 since these factors function as angiogenesis inhibitors and can thus contribute to the phenotype observed *in vivo*.

Further studies using *in situ* hybridization indicated that Jagged1, Dll4, Notch3 and Hes1 expression is not regulated by catalase overexpression as the expression of these genes was

not concomitant with catalase overexpressing cells. However, more studies are needed to determine whether Notch signaling components could be regulated by H_2O_2 levels in a non-autonomous way.

Recently, Notch3 was found to be upregulated and required for tumor cell propagation on a subpopulation of non-small-cell-lung cancer with cancer stem cell properties (Zheng, de la Cruz et al. 2013) such as resistance to chemotherapy.

As CSCs have been described as having low levels of ROS (Diehn, Cho et al. 2009), the relation between ROS, Notch expression and these tumor promoting cells may prove to be important for future therapeutic strategies.

2. CELL AUTONOMOUS VS NON-AUTONOMOUS H_2O_2 EFFECT

Bai1 expression was not detected by qRT-PCR or immunofluorescence, which was probably due to very low expression of this gene, forfeiting us the possibility of further studies.

For Thbs1, a significant increase was found in number of Thbs1 positive cells in catalase overexpressing cell cultures when compared to controls. Yet the Thbs1 positive cells showed no correspondence with catalase overexpressing cells as observed using immunofluorescence, showing a non-autonomous effect.

An increase, although not significant, was found in cells incubated with conditioned media from catalase overexpressing cells when compared with conditioned media from control cells. These results suggest that Thbs1 expression is controlled by extracellular factors induced by alterations in H_2O_2 levels in a small subpopulation of tumor cells.

H_2O_2 reacts with and modulates the activity of several factors including signaling molecules and redox sensitive transcription factors, as previously described.

We hypothesize that redox changes caused by catalase overexpressing affects the expression or activity of a secondary messenger responsible for Thbs1 induction. An increase in the expression or activity of such messenger would happen in conditioned media from catalase overexpressing cells.

Timp3 immunofluorescence, in contrast to Thbs1, showed an increase in Timp3 expression which is specific to catalase overexpressing cells. Assays with conditioned media and extracellular catalase were also performed and no Timp3 expression was observed in either case, confirming the cell autonomous effect of H_2O_2.

H_2O_2 regulates expression at the transcription, translation and protein degradation levels but is also a key factor in signal transduction of extracellular factors.

Timp3 regulation by H_2O_2 may occur at one or more of these levels. Timp3 downregulation has been linked to hypermethylation of its promoter in several cancers including invasive breast ductal cancer (Lui, E. L. H. et al 2005). In addition, Timp3 transcription is known to be induced by TGF-β and TNF-α signaling, and the downstream signaling of both these factors is modulated by H_2O_2 (Khokha, Murthy et al. 2013). The possibility that the increase in intracellular Timp3 is due to deficient exocytosis cannot be discarded and will be investigated in subsequent studies.

The possible targets of H_2O_2 that have been found will need further confirmation.

Of particular interest is the determination of overall expression changes in the notch pathway components in control and CatO populations, as it may have a non-autonomous effect. Determination of intermediates regulating Thbs1 and Timp3 expressing by analysis of changes in the conditioned media and inhibition of signal transduction component, respectively.

The expression of these molecules should also be confirmed in an *in vivo* scenario which includes other determining factors in the tumor microenvironment, to understand their importance in the phenotype.

The levels of endogenous H_2O_2 in endothelial cells are also a key factor in the angiogenic process. However, it is still unknown whether H_2O_2 regulates both physiological and pathological angiogenesis and in which stages of this process it could be determinant.

To answer this questions we aim at creating a Zebrafish transgenic line that allows the inducible expression of catalase in endothelial cells by addition of the drug tamoxifen. This will allow the manipulation of H_2O_2 levels at different time points of the angiogenic process thus elucidating the different phases of this process.

CONCLUSIONS

The present work was aimed at identifying H_2O_2 regulated factors responsible for a decrease in tumor induced angiogenesis, observed when a subset of 4T1 tumor cells was transfected with a catalase overexpression plasmid in a Zebrafish xenograft model.

Expression changes which may contribute to the observed phenotype were found in components of the Notch signaling pathway and molecules with antiangiogenic properties, namely Bai1, Thbs1 and Timp3.

We observed that Dll4, Jagged1, Notch3 and Hes1 are expressed in 4T1, that this expression happened in both control and CatO cells and there was no apparent relation between the reduction of H_2O_2 levels and Notch pathway induction.

We also found that the expression of Thbs1 and Timp3 was regulated by H_2O_2 in distinct ways: non-autonomously and autonomously.

While Timp3 was upregulated specifically in cells overexpressing catalase, Thbs1 expression did not correlate in an autonomous way with catalase overexpression but presented a higher percentage of Thbs1 positive cells in CatO cell cultures and cells incubated with CatO cell culture conditioned media suggesting the role of a second messenger.

Included in a broader study plan, this work also encompassed making a construct that will allow the creation of a Zebrafish transgenic expressing catalase in endothelial cells at specific times during angiogenesis by induction using tamoxifen.

PERSPECTIVES

To better understand the relevance and mechanisms of these angiogenic factors more assays are needed to confirm these results as well as new assays to characterize the way H_2O_2 performs this regulation

Different pathways, such as MAPK and PI3K, may be inhibited to determine their involvement in the regulation process and other processes such as exocytosis of Timp3 may be analyzed.

To understand whether the redox regulation uncovered in this study has *in vivo* relevance we will use the zebrafish tumor model optimized previously to analyze the expression of the H_2O_2-regulated proteins here identified.

SUPPLEMENTARY MATERIALS

Table 16

Angiogenesis related genes differently expressed in controls and catalase overexpressing 4T1 cells

Symbol	Function in angiogenesis	Uniprot number	References
Bai1	Brain-specific angiogenesis inhibitor 1 is a G-coupled protein receptor of the cell adhesion subfamily containing five thrombospondin type I repeats. Cleavage of its extracellular domain results in two molecules, vasculostatin 120 and vasculostatin 40, with strong antiangiogenic properties.	Q3UHD1	Cork and Van Meir 2011
Cga	Glycoprotein hormones, alpha subunit is a subunit of several hormones involved in fetal angiogenesis. Its folding and secretion is dependent upon bonds between cysteine residues	P01216	Tsampalas et al., 2010
Chga	Chromogranin A is a secretory protein used as a diagnostic serum marker for neuroendocrine tumors. The N-terminal fragment of Chromogranin A is the anti-angiogenic molecule Vasostatin I which reduces endothelial cell proliferation and migration.	P26339	Belloni, Scabini et al. 2007
Col4a3	Collagen, type IV, alpha 3 has a proteolytic C-terminal non-collagenous (NC1) domain that is released by membrane degrading enzymes forming Tumstatin, an endogenous inhibitor of angiogenesis.	Q9QZS0	Boosani, C.S. and Sudhakar, A., 2008
Hey1	Hairy/enhancer-of-split related with YRPW motif 1 is a Notch effector, involved in tip vs stalk cell selection and tumor and endothelial cell crosstalk	Q9WV93	Kofler, N.M. et al, 2011
Hey2	Hairy/enhancer-of-split related with YRPW motif 2 is a Notch effector, involved in tip vs stalk cell selection and tumor and endothelial cell crosstalk	Q9QUS4	
IL12a	Interleukin 12A and 12B form the Interleukin12 heterodimer that acts as angiogenesis inhibitor. However, this activity is mediated by regulating interferon γ and CXCL10 and expression levels of these were found to be unchanged.	P43431	Angiolillo AL et al, 1996
Ntrk2	Neurotrophic tyrosine kinase, receptor, type 2 is involved in signal transduction cascades that regulate growth and survival and was associated with the expressions of VEGF, VEGF-C and VEGF-D	P15209	(Sasahira, Ueda et al. 2013)

Prl7d1	Prolactin family 7, subfamily d, member 1 is a hormone expressed mainly in the placenta and mammary gland involved in many cellular processes. Fragments of this hormone have been shown to have antiangiogenic activity.	Q5SVM4	Jackson et al, 1994
Plg	Plasminogen is a precursor to plasmin, a molecule that is reduced extracellularly and then cleaved to the potent angiogenesis inhibitor angiostatin	P20918	Gately S. et al 1997 Stathakis P. et al 1999
Ptn	Pleiotrophin is a secreted heparin binding cytokine. It has strong pro-angiogenic effects through EC stimulation, signaling pathway activation and stromal alterations.	P63089	Perez-Pinera, Chang et al. 2007
Tdgf1	Teratocarcinoma-derived growth factor 1 is an embryonic growth factor generally absent in adult tissues but known to be present in some tumors where it interacts with a variety of proteins in signaling pathways that drive tumorigenesis, including angiogenesis.	P51865	de Castro, Rangel et al. 2010 Nagaoka, Karasawa et al. 2012
Thbs1	Thrombospondin 1 is a glycoprotein with multiple functional domains that can interact with constituents of the ECM, proteases and cell receptors. Its antitumorigenic and antiangiogenic properties have been thoroughly studied and established.	P35441	Tuszynski and Nicosia 1996 Lawler and Lawler 2012
Timp3	Tissue inhibitor of metalloproteinase 3 is part of a family of endogenous antiangiogenic factors that act by inhibiting MMPs. Its binding to MMPs prevents ECM degradation and the release of proangiogenic molecules. It has also been shown to block VEGF binding to VEGFR2, independently of its timp function.	P39876	Apte, Olsen et al. 1995 Qi, Ebrahem et al. 2003
Timp4	Tissue inhibitor of metalloproteinase 4 is also part of the family of endogenous antiangiogenic factors that inhibit MMPs. Similarly to Timp3, it binds to MMPs to prevent ECM degradation.	Q9JHB3	Apte, Olsen et al. 1995

BIBLIOGRAPHY

Abate, C., L. Patel, F. J. Rauscher, 3rd and T. Curran (1990). "Redox regulation of fos and jun DNA-binding activity in vitro." Science **249**(4973): 1157-1161.

Abid, M. R., K. C. Spokes, S. C. Shih and W. C. Aird (2007). "NADPH oxidase activity selectively modulates vascular endothelial growth factor signaling pathways." J Biol Chem **282**(48): 35373-35385.

Angiolillo AL, Sgadari C, Tosato G (1996) A role for the interferon-inducible protein 10 in inhibition of angiogenesis by interleukin-12. Ann N Y Acad Sci 795: 158–167

Almendro, V., A. Marusyk and K. Polyak (2013). "Cellular heterogeneity and molecular evolution in cancer." Annu Rev Pathol **8**: 277-302.

Apte, S. S., B. R. Olsen and G. Murphy (1995). "The gene structure of tissue inhibitor of metalloproteinases (TIMP)-3 and its inhibitory activities define the distinct TIMP gene family." J Biol Chem **270**(24): 14313-14318.

Belloni, D., S. Scabini, C. Foglieni, L. Veschini, A. Giazzon, B. Colombo, A. Fulgenzi, K. B. Helle, M. E. Ferrero, A. Corti and E. Ferrero (2007). "The vasostatin-I fragment of chromogranin A inhibits VEGF-induced endothelial cell proliferation and migration." FASEB J **21**(12): 3052-3062.

Bertout, J. A., S. A. Patel and M. C. Simon (2008). "The impact of O2 availability on human cancer." Nat Rev Cancer **8**(12): 967-975.

Bradford, M. M. (1976). "A rapid and sensitive method for the quantitation of microgram quantities of protein utilizing the principle of protein-dye binding." Anal Biochem **72**: 248-254.

Brown, M. R., F. J. Miller, Jr., W. G. Li, A. N. Ellingson, J. D. Mozena, P. Chatterjee, J. F. Engelhardt, R. M. Zwacka, L. W. Oberley, X. Fang, A. A. Spector and N. L. Weintraub (1999). "Overexpression of human catalase inhibits proliferation and promotes apoptosis in vascular smooth muscle cells." Circ Res **85**(6): 524-533.

Brunelle, J. K., E. L. Bell, N. M. Quesada, K. Vercauteren, V. Tiranti, M. Zeviani, R. C. Scarpulla and N. S. Chandel (2005). "Oxygen sensing requires mitochondrial ROS but not oxidative phosphorylation." Cell Metab **1**(6): 409-414.

Burdon, R. H. (1995). "Superoxide and hydrogen peroxide in relation to mammalian cell proliferation." Free Radic Biol Med **18**(4): 775-794.

Cairns, R. A., I. S. Harris and T. W. Mak (2011). "Regulation of cancer cell metabolism." Nat Rev Cancer **11**(2): 85-95.

Carmeliet, P. (2003). "Angiogenesis in health and disease." Nat Med **9**(6): 653-660.

Carmeliet, P. and R. K. Jain (2011). "Molecular mechanisms and clinical applications of angiogenesis." Nature **473**(7347): 298-307.

Ceccarelli, J., L. Delfino, E. Zappia, P. Castellani, M. Borghi, S. Ferrini, F. Tosetti and A. Rubartelli (2008). "The redox state of the lung cancer microenvironment depends on the levels of thioredoxin expressed by tumor cells and affects tumor progression and response to prooxidants." Int J Cancer **123**(8): 1770-1778.

Chiche, J., M. C. Brahimi-Horn and J. Pouyssegur (2010). "Tumour hypoxia induces a metabolic shift causing acidosis: a common feature in cancer." J Cell Mol Med **14**(4): 771-794.

Chung, C. C., W. C. Magalhaes, J. Gonzalez-Bosquet and S. J. Chanock (2010). "Genome-wide association studies in cancer--current and future directions." Carcinogenesis **31**(1): 111-120.

Clapp, C., S. Thebault, M. C. Jeziorski and G. Martinez De La Escalera (2009). "Peptide hormone regulation of angiogenesis." Physiol Rev **89**(4): 1177-1215.

Cook, K. M. and P. J. Hogg (2013). "Post-translational control of protein function by disulfide bond cleavage." Antioxid Redox Signal **18**(15): 1987-2015.

Cork, S. M. and E. G. Van Meir (2011). "Emerging roles for the BAI1 protein family in the regulation of phagocytosis, synaptogenesis, neurovasculature, and tumor development." J Mol Med (Berl) **89**(8): 743-752.

Coussens, L. M. and Z. Werb (2002). "Inflammation and cancer." Nature **420**(6917): 860-867.

D'Autreaux, B. and M. B. Toledano (2007). "ROS as signalling molecules: mechanisms that generate specificity in ROS homeostasis." Nat Rev Mol Cell Biol **8**(10): 813-824.

DeBerardinis, R. J. (2012). "Good neighbours in the tumour stroma reduce oxidative stress." Nat Cell Biol **14**(3): 235-236.

de Castro, N. P., M. C. Rangel, T. Nagaoka, D. S. Salomon and C. Bianco (2010). "Cripto-1: an embryonic gene that promotes tumorigenesis." Future Oncol **6**(7): 1127-1142.

Diehn, M., R. W. Cho, N. A. Lobo, T. Kalisky, M. J. Dorie, A. N. Kulp, D. Qian, J. S. Lam, L. E. Ailles, M. Wong, B. Joshua, M. J. Kaplan, I. Wapnir, F. M. Dirbas, G. Somlo, C. Garberoglio, B. Paz, J. Shen, S. K. Lau, S. R. Quake, J. M. Brown, I. L. Weissman and M. F. Clarke (2009). "Association of reactive oxygen species levels and radioresistance in cancer stem cells." Nature **458**(7239): 780-783.

Distel, M., M. F. Wullimann and R. W. Koster (2009). "Optimized Gal4 genetics for permanent gene expression mapping in zebrafish." Proc Natl Acad Sci U S A **106**(32): 13365-13370.

Drose, S. and U. Brandt (2012). "Molecular mechanisms of superoxide production by the mitochondrial respiratory chain." Adv Exp Med Biol **748**: 145-169.

Dvorak, H. F. (1986). "Tumors: wounds that do not heal. Similarities between tumor stroma generation and wound healing." N Engl J Med **315**(26): 1650-1659.

Evans, M. D., M. Dizdaroglu and M. S. Cooke (2004). "Oxidative DNA damage and disease: induction, repair and significance." Mutat Res **567**(1): 1-61.

Fang, J., H. Nakamura and A. K. Iyer (2007). "Tumor-targeted induction of oxystress for cancer therapy." J Drug Target **15**(7-8): 475-486.

Feng, Y., C. Santoriello, M. Mione, A. Hurlstone and P. Martin (2010). "Live imaging of innate immune cell sensing of transformed cells in zebrafish larvae: parallels between tumor initiation and wound inflammation." PLoS Biol **8**(12): e1000562.

Ferrara, N., H. P. Gerber and J. LeCouter (2003). "The biology of VEGF and its receptors." Nat Med **9**(6): 669-676.

Ferrara, N., K. J. Hillan, H. P. Gerber and W. Novotny (2004). "Discovery and development of bevacizumab, an anti-VEGF antibody for treating cancer." Nat Rev Drug Discov **3**(5): 391-400.

Finkel, T. (2011). "Signal transduction by reactive oxygen species." J Cell Biol **194**(1): 7-15.

Flohe, L., R. Brigelius-Flohe, C. Saliou, M. G. Traber and L. Packer (1997). "Redox regulation of NF-kappa B activation." Free Radic Biol Med **22**(6): 1115-1126.

Folkman, J. (1974). "Tumor angiogensis: role in regulation of tumor growth." Symp Soc Dev Biol **30**(0): 43-52.

Franco, O. E., A. K. Shaw, D. W. Strand and S. W. Hayward (2010). "Cancer associated fibroblasts in cancer pathogenesis." Semin Cell Dev Biol **21**(1): 33-39.

Garcia-Roman, J. and A. Zentella-Dehesa (2013). "Vascular permeability changes involved in tumor metastasis." Cancer Lett **335**(2): 259-269.

Gately S, Twardowski P, Stack MS, Cundiff DL, Grella D, Castellino FJ, et al. The mechanism of cancer-mediated conversion of plasminogen to the angiogenesis inhibitor angiostatin. Proc Natl Acad Sci U S A.1997 Sep 30;94(20):10868–72

Gatenby, R. A., E. T. Gawlinski, A. F. Gmitro, B. Kaylor and R. J. Gillies (2006). "Acid-mediated tumor invasion: a multidisciplinary study." Cancer Res **66**(10): 5216-5223.

Glorieux, C., N. Dejeans, B. Sid, R. Beck, P. B. Calderon and J. Verrax (2011). "Catalase overexpression in mammary cancer cells leads to a less aggressive phenotype and an altered response to chemotherapy." Biochem Pharmacol **82**(10): 1384-1390.

Goh, J., L. Enns, S. Fatemie, H. Hopkins, J. Morton, C. Pettan-Brewer and W. Ladiges (2011). "Mitochondrial targeted catalase suppresses invasive breast cancer in mice." BMC Cancer **11**: 191.

Goitre, L., B. Pergolizzi, E. Ferro, L. Trabalzini and S. F. Retta (2012). "Molecular Crosstalk between Integrins and Cadherins: Do Reactive Oxygen Species Set the Talk?" J Signal Transduct **2012**: 807682.

Graham, K. A., M. Kulawiec, K. M. Owens, X. Li, M. M. Desouki, D. Chandra and K. K. Singh (2010). "NADPH oxidase 4 is an oncoprotein localized to mitochondria." Cancer Biol Ther **10**(3): 223-231.

Hanahan, D. and R. A. Weinberg (2011). "Hallmarks of cancer: the next generation." Cell **144**(5): 646-674.

Hans, S., J. Kaslin, D. Freudenreich and M. Brand (2009). "Temporally-controlled site-specific recombination in zebrafish." PLoS One **4**(2): e4640.

Harfouche, R., N. A. Malak, R. P. Brandes, A. Karsan, K. Irani and S. N. Hussain (2005). "Roles of reactive oxygen species in angiopoietin-1/tie-2 receptor signaling." FASEB J **19**(12): 1728-1730.

He, J., Q. Xu, Y. Jing, F. Agani, X. Qian, R. Carpenter, Q. Li, X. R. Wang, S. S. Peiper, Z. Lu, L. Z. Liu and B. H. Jiang (2012). "Reactive oxygen species regulate ERBB2 and ERBB3 expression via miR-199a/125b and DNA methylation." EMBO Rep **13**(12): 1116-1122.

Herbert, S. P. and D. Y. Stainier (2011). "Molecular control of endothelial cell behaviour during blood vessel morphogenesis." Nat Rev Mol Cell Biol **12**(9): 551-564.

Hodara, R., D. Weiss, G. Joseph, J. C. Velasquez-Castano, N. Landazuri, J. W. Han, Y. S. Yoon and W. R. Taylor (2011). "Overexpression of catalase in myeloid cells causes impaired postischemic neovascularization." Arterioscler Thromb Vasc Biol **31**(10): 2203-2209.

Hurd, T. R., M. DeGennaro and R. Lehmann (2012). "Redox regulation of cell migration and adhesion." Trends Cell Biol **22**(2): 107-115.

Inoue, H., H. Nojima and H. Okayama (1990). "High efficiency transformation of Escherichia coli with plasmids." Gene **96**(1): 23-28.

Ishikawa, K., K. Takenaga, M. Akimoto, N. Koshikawa, A. Yamaguchi, H. Imanishi, K. Nakada, Y. Honma and J. Hayashi (2008). "ROS-generating mitochondrial DNA mutations can regulate tumor cell metastasis." Science **320**(5876): 661-664.

Ivanovic, Z. (2009). "Hypoxia or in situ normoxia: The stem cell paradigm." J Cell Physiol **219**(2): 271-275.

Jackson D., Volpert O. V., Bouck N., Linzer D. I. (1994) Stimulation and inhibition of angiogenesis by placental proliferin and proliferin-related protein. Science 266, 1581–1584

Jemal, A., F. Bray, M. M. Center, J. Ferlay, E. Ward and D. Forman (2011). "Global cancer statistics." CA Cancer J Clin **61**(2): 69-90.

Jin, B. Y., A. J. Lin, D. E. Golan and T. Michel (2012). "MARCKS protein mediates hydrogen peroxide regulation of endothelial permeability." Proc Natl Acad Sci U S A **109**(37): 14864-14869.

Jorgenson, T. C., W. Zhong and T. D. Oberley (2013). "Redox imbalance and biochemical changes in cancer." Cancer Res **73**(20): 6118-6123.

Kaelin, W. G., Jr. (2002). "Molecular basis of the VHL hereditary cancer syndrome." Nat Rev Cancer **2**(9): 673-682.

Kang, K. A., R. Zhang, G. Y. Kim, S. C. Bae and J. W. Hyun (2012). "Epigenetic changes induced by oxidative stress in colorectal cancer cells: methylation of tumor suppressor RUNX3." Tumour Biol **33**(2): 403-412.

Kang, S. W., S. G. Rhee, T. S. Chang, W. Jeong and M. H. Choi (2005). "2-Cys peroxiredoxin function in intracellular signal transduction: therapeutic implications." Trends Mol Med **11**(12): 571-578.

Kansanen, E., S. M. Kuosmanen, H. Leinonen and A. L. Levonen (2013). "The Keap1-Nrf2 pathway: Mechanisms of activation and dysregulation in cancer." Redox Biol **1**(1): 45-49.

Kao, Y. Y., D. Gianni, B. Bohl, R. M. Taylor and G. M. Bokoch (2008). "Identification of a conserved Rac-binding site on NADPH oxidases supports a direct GTPase regulatory mechanism." J Biol Chem **283**(19): 12736-12746.

Karihtala, P., S. Kauppila, Y. Soini and V. Arja Jukkola (2011). "Oxidative stress and counteracting mechanisms in hormone receptor positive, triple-negative and basal-like breast carcinomas." BMC Cancer **11**: 262.

Katsuyuki, M., N. Kohzo, F. Kotaro, S. Xiangao, S. Shuji and Y. Ken-ichi (1994). "Two different cellular redox systems regulate the DNA-binding activity of the p50 subunit of NF-κB in vitro." Gene **145**(2): 197-203.

Keith, B., R. S. Johnson and M. C. Simon (2012). "HIF1alpha and HIF2alpha: sibling rivalry in hypoxic tumour growth and progression." Nat Rev Cancer **12**(1): 9-22.

Khokha, R., A. Murthy and A. Weiss (2013). "Metalloproteinases and their natural inhibitors in inflammation and immunity." Nat Rev Immunol **13**(9): 649-665.

Kodydkova, J., L. Vavrova, B. Stankova, J. Macasek, T. Krechler and A. Zak (2013). "Antioxidant status and oxidative stress markers in pancreatic cancer and chronic pancreatitis." Pancreas **42**(4): 614-621.

Kofler NM, Shawber CJ, Kangsamaksin T, Reed HO, Galatioto J, et al. (2011) Notch signaling in developmental and tumor angiogenesis. Genes Cancer 2: 1106–1116

Kumar, B., S. Koul, L. Khandrika, R. B. Meacham and H. K. Koul (2008). "Oxidative stress is inherent in prostate cancer cells and is required for aggressive phenotype." Cancer Res **68**(6): 1777-1785.

Lawler, P. R. and J. Lawler (2012). "Molecular basis for the regulation of angiogenesis by thrombospondin-1 and -2." Cold Spring Harb Perspect Med **2**(5): a006627.

Lim, S. O., J. M. Gu, M. S. Kim, H. S. Kim, Y. N. Park, C. K. Park, J. W. Cho, Y. M. Park and G. Jung (2008). "Epigenetic changes induced by reactive oxygen species in hepatocellular carcinoma: methylation of the E-cadherin promoter." Gastroenterology **135**(6): 2128-2140, 2140 e2121-2128.

Liu, S. and S. D. Leach (2011). "Zebrafish models for cancer." Annu Rev Pathol **6**: 71-93.

Lopez-Lazaro, M. (2007). "Dual role of hydrogen peroxide in cancer: possible relevance to cancer chemoprevention and therapy." Cancer Lett **252**(1): 1-8.

Lu, P., V. M. Weaver and Z. Werb (2012). "The extracellular matrix: a dynamic niche in cancer progression." J Cell Biol **196**(4): 395-406.

Malik, B. and D. Nie (2012). "Cancer stem cells and resistance to chemo and radio therapy." Front Biosci (Elite Ed) **4**: 2142-2149.

Maniatis, T., E. F. Fritsch and J. Sambrook (1982). Molecular cloning: a laboratory manual, Cold Spring Harbor Laboratory.

McEarchern, J. A., J. J. Kobie, V. Mack, R. S. Wu, L. Meade-Tollin, C. L. Arteaga, N. Dumont, D. Besselsen, E. Seftor, M. J. Hendrix, E. Katsanis and E. T. Akporiaye (2001). "Invasion and metastasis of a mammary tumor involves TGF-beta signaling." Int J Cancer **91**(1): 76-82.

Melo, A., L. Monteiro, R. M. Lima, D. M. Oliveira, M. D. Cerqueira and R. S. El-Bacha (2011). "Oxidative stress in neurodegenerative diseases: mechanisms and therapeutic perspectives." Oxid Med Cell Longev **2011**: 467180.

Min, J. Y., S. O. Lim and G. Jung (2010). "Downregulation of catalase by reactive oxygen species via hypermethylation of CpG island II on the catalase promoter." FEBS Lett **584**(11): 2427-2432.

Negrini, S., V. G. Gorgoulis and T. D. Halazonetis (2010). "Genomic instability--an evolving hallmark of cancer." Nat Rev Mol Cell Biol **11**(3): 220-228.

Nicoli, S. and M. Presta (2007). "The zebrafish/tumor xenograft angiogenesis assay." Nat Protoc **2**(11): 2918-2923.

Niethammer, P., C. Grabher, A. T. Look and T. J. Mitchison (2009). "A tissue-scale gradient of hydrogen peroxide mediates rapid wound detection in zebrafish." Nature **459**(7249): 996-999.

Oliveira-Marques, V., Marinho, H.S., Cyrne, L. & Antunes, F. (2009) Role of hydrogen peroxide in NF-kB activation: from inducer to modulator. *Antioxid. Redox Signal.*, **11**, 2223-2243

Owegi, H. O., S. Egot-Lemaire, L. R. Waite and G. N. Waite (2010). "Macrophage activity in response to steady-state oxygen and hydrogen peroxide concentration - biomed 2010." Biomed Sci Instrum **46**: 57-62.

Perez-Pinera, P., Y. Chang and T. F. Deuel (2007). "Pleiotrophin, a multifunctional tumor promoter through induction of tumor angiogenesis, remodeling of the tumor microenvironment, and activation of stromal fibroblasts." Cell Cycle **6**(23): 2877-2883.

Qi, J. H., Q. Ebrahem, N. Moore, G. Murphy, L. Claesson-Welsh, M. Bond, A. Baker and B. Anand-Apte (2003). "A novel function for tissue inhibitor of metalloproteinases-3 (TIMP3): inhibition of angiogenesis by blockage of VEGF binding to VEGF receptor-2." Nat Med **9**(4): 407-415.

Qutub, A. A. and A. S. Popel (2008). "Reactive oxygen species regulate hypoxia-inducible factor 1alpha differentially in cancer and ischemia." Mol Cell Biol **28**(16): 5106-5119.

Radisky, D. C., D. D. Levy, L. E. Littlepage, H. Liu, C. M. Nelson, J. E. Fata, D. Leake, E. L. Godden, D. G. Albertson, M. A. Nieto, Z. Werb and M. J. Bissell (2005). "Rac1b and reactive oxygen species mediate MMP-3-induced EMT and genomic instability." Nature **436**(7047): 123-127.

Rak, J., J. L. Yu, G. Klement and R. S. Kerbel (2000). "Oncogenes and angiogenesis: signaling three-dimensional tumor growth." J Investig Dermatol Symp Proc **5**(1): 24-33.

Rhyu, D. Y., Y. Yang, H. Ha, G. T. Lee, J. S. Song, S. T. Uh and H. B. Lee (2005). "Role of reactive oxygen species in TGF-beta1-induced mitogen-activated protein kinase activation and epithelial-mesenchymal transition in renal tubular epithelial cells." J Am Soc Nephrol **16**(3): 667-675.

Risau, W. and I. Flamme (1995). "Vasculogenesis." Annu Rev Cell Dev Biol **11**: 73-91.

Rousseau, S., F. Houle, J. Landry and J. Huot (1997). "p38 MAP kinase activation by vascular endothelial growth factor mediates actin reorganization and cell migration in human endothelial cells." Oncogene **15**(18): 2169-2177.

Samper, E., D. G. Nicholls and S. Melov (2003). "Mitochondrial oxidative stress causes chromosomal instability of mouse embryonic fibroblasts." Aging Cell **2**(5): 277-285.

Sasahira, T., N. Ueda, K. Yamamoto, U. Bhawal, M. Kurihara, T. Kirita and H. Kuniyasu (2013). "Trks are novel oncogenes involved in the induction of neovascularization, tumor progression, and nodal metastasis in oral squamous cell carcinoma." Clinical & Experimental Metastasis **30**(2): 165-176.

Semenza, G. L. (2003). "Targeting HIF-1 for cancer therapy." Nat Rev Cancer **3**(10): 721-732.

Siegel, R., D. Naishadham and A. Jemal (2012). "Cancer statistics, 2012." CA Cancer J Clin **62**(1): 10-29.

Sigaud, S., P. Evelson and B. Gonzalez-Flecha (2005). "H2O2-induced proliferation of primary alveolar epithelial cells is mediated by MAP kinases." Antioxid Redox Signal **7**(1-2): 6-13.

Son, Y., Y. K. Cheong, N. H. Kim, H. T. Chung, D. G. Kang and H. O. Pae (2011). "Mitogen-Activated Protein Kinases and Reactive Oxygen Species: How Can ROS Activate MAPK Pathways?" J Signal Transduct **2011**: 792639.

Stathakis P., Lay A. J., Fitzgerald M., Schlieker C., Matthias L. J., Hogg P. J. (1999) J. Biol. Chem. 274, 8910–8916

Sudhakar A, Boosani CS. Inhibition of tumor angiogenesis by tumstatin: insights into signaling mechanisms and implications in cancer regression. Pharm Res. 2008;25:2731–9

Suzuki, Y., K. Imai, K. Takai, T. Hanai, H. Hayashi, T. Naiki, Y. Nishigaki, E. Tomita, M. Shimizu and H. Moriwaki (2013). "Hepatocellular carcinoma patients with increased oxidative stress levels are prone to recurrence after curative treatment: a prospective case series study using the d-ROM test." J Cancer Res Clin Oncol **139**(5): 845-852.

Szatrowski, T. P. and C. F. Nathan (1991). "Production of large amounts of hydrogen peroxide by human tumor cells." Cancer Res **51**(3): 794-798.

Thimmulappa, R. K., K. H. Mai, S. Srisuma, T. W. Kensler, M. Yamamoto and S. Biswal (2002). "Identification of Nrf2-regulated genes induced by the chemopreventive agent sulforaphane by oligonucleotide microarray." Cancer Res **62**(18): 5196-5203.

Tochhawng, L., S. Deng, S. Pervaiz and C. T. Yap (2013). "Redox regulation of cancer cell migration and invasion." Mitochondrion **13**(3): 246-253.

Trachootham, D., J. Alexandre and P. Huang (2009). "Targeting cancer cells by ROS-mediated mechanisms: a radical therapeutic approach?" Nat Rev Drug Discov **8**(7): 579-591.

Truong, T. H. and K. S. Carroll (2012). "Redox regulation of epidermal growth factor receptor signaling through cysteine oxidation." Biochemistry **51**(50): 9954-9965.

Tsampalas M, Gridelet V, Berndt S, Foidart JM, Geenen V, Perrier d'Hauterive S. Human chorionic gonadotropin: a hormone with immunological and angiogenic properties. J Reprod Immunol. 2010;85(1):93–8

Urasaki, A., G. Morvan and K. Kawakami (2006). "Functional dissection of the Tol2 transposable element identified the minimal cis-sequence and a highly repetitive sequence in the subterminal region essential for transposition." Genetics **174**(2): 639-649.

Ushio-Fukai, M. (2006). "Redox signaling in angiogenesis: role of NADPH oxidase." Cardiovasc Res **71**(2): 226-235.

Weiss, S. J., G. Peppin, X. Ortiz, C. Ragsdale and S. T. Test (1985). "Oxidative autoactivation of latent collagenase by human neutrophils." Science **227**(4688): 747-749.

Weydert, C. J. and J. J. Cullen (2010). "Measurement of superoxide dismutase, catalase and glutathione peroxidase in cultured cells and tissue." Nat Protoc **5**(1): 51-66.

Weydert, C. J., T. A. Waugh, J. M. Ritchie, K. S. Iyer, J. L. Smith, L. Li, D. R. Spitz and L. W. Oberley (2006). "Overexpression of manganese or copper-zinc superoxide dismutase inhibits breast cancer growth." Free Radic Biol Med **41**(2): 226-237.

Woo, H. A., S. H. Yim, D. H. Shin, D. Kang, D. Y. Yu and S. G. Rhee (2010). "Inactivation of peroxiredoxin I by phosphorylation allows localized H(2)O(2) accumulation for cell signaling." Cell **140**(4): 517-528.

Wu, W. S. (2006). "The signaling mechanism of ROS in tumor progression." Cancer Metastasis Rev **25**(4): 695-705.

Yang, L. (2010). "TGFbeta, a potent regulator of tumor microenvironment and host immune response, implication for therapy." Curr Mol Med **10**(4): 374-380.

Zanetti, M., Z. S. Katusic and T. O'Brien (2002). "Adenoviral-mediated overexpression of catalase inhibits endothelial cell proliferation." Am J Physiol Heart Circ Physiol **283**(6): H2620-2626.

Zhang, R., K. A. Kang, K. C. Kim, S. Y. Na, W. Y. Chang, G. Y. Kim, H. S. Kim and J. W. Hyun (2013). "Oxidative stress causes epigenetic alteration of CDX1 expression in colorectal cancer cells." Gene **524**(2): 214-219.

Zhang, Y., W. Zhao, H. J. Zhang, F. E. Domann and L. W. Oberley (2002). "Overexpression of copper zinc superoxide dismutase suppresses human glioma cell growth." Cancer Res **62**(4): 1205-1212.

Zheng, Y., Cecile C. de la Cruz, Leanne C. Sayles, C. Alleyne-Chin, D. Vaka, Tim D. Knaak, M. Bigos, Y. Xu, Chuong D. Hoang, Joseph B. Shrager, Hans J. Fehling, D. French, W. Forrest, Z. Jiang, R. A. D. Carano, K. H. Barck, Erica L. Jackson and E. A. Sweet-Cordero (2013). "A Rare Population of CD24+ITGB4+Notchhi Cells Drives Tumor Propagation in NSCLC and Requires Notch3 for Self-Renewal." Cancer Cell **24**(1): 59-74.

Zhou, Y., H. Yan, M. Guo, J. Zhu, Q. Xiao and L. Zhang (2013). "Reactive oxygen species in vascular formation and development." Oxid Med Cell Longev **2013**: 374963.

Ziech, D., R. Franco, A. Pappa and M. I. Panayiotidis (2011). "Reactive oxygen species (ROS)--induced genetic and epigenetic alterations in human carcinogenesis." Mutat Res **711**(1-2): 167-173.